Tertiary Carbonate Side Chains: Easily Tuneable Thermo-Labile Breaking Points for Controlling the Solubility of Conjugated Polymers

SCHOLARONE™
Manuscripts

Tertiary Carbonate Side Chains: Easily Tuneable Thermo-Labile Breaking Points for Controlling the Solubility of Conjugated Polymers

Marius Kuhn,[a)d)] Jens Ludwig,[b)] Tomasz Marszalek,[c)] Torben Adermann,[a)d)] Wojciech Pisula,[c)] Klaus Müllen,[c)d)] Alexander Colsmann,[b)] Manuel Hamburger[a)d)]*

a) Institute of Organic Chemistry, Heidelberg University, Im Neuenheimer Feld 270, 69120 Heidelberg, Germany

b) Light Technology Institute, Karlsruhe Institute of Technology (KIT), Engesserstrasse 13, 76131 Karlsruhe, Germany

c) Max Planck Institute for Polymer Research, Ackermannweg 10, 55128 Mainz, Germany

d) InnovationLab GmbH, Speyerer Strasse 4, 69115 Heidelberg, Germany

Abstract

Breakpoints are not exclusive to tennis: We present a new class of solubilizing groups for conjugated polymers which enable solution processing of multi-layer devices. Conjugated polymers in organic devices are sometimes difficult to process due to their limited solubility. Well soluble polymers decorated with alkyl side chains, however, introduce new challenges for thin-film deposition: Using the same solvent for multiple layers can dissolve the already applied layers. In this work we introduce a new class of thermo-labile groups which reduce the solubility of conjugated polymers after thermal treatment. Following a very modular approach, we can tune the temperature of the thermo-cleavage between 140 and 200 °C. This enables the fabrication of organic solar cells and field-effect transistors (FETs) with robust, solvent-resistant active layers.
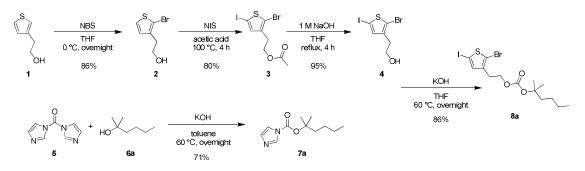
1. Introduction

The unique optical, electrical, and film-forming properties of π-conjugated polymers enable various optoelectronic applications.[1] However, using soluble polymers opens new processing challenges for the fabrication of more sophisticated device architectures. To make conjugated organic materials solution-processable, the introduction of solubilizing groups is often necessary,[2] although these groups can dramatically influence the solid-state structure of these compounds (e.g. their overall crystallinity or packing).[3,4,5,6] It is hardly possible to use the same or similar solvents for the deposition of consecutive layers, because of the dissolution of the layers that were already applied. Different approaches addressed this issue which are based on crosslinking,[7,8] the use of orthogonal solvents,[9,10] or treatment with an external stimulus, such as heat,[11,12,13] all to prevent the dissolution of the previously formed layers. Especially, the treatment of the processed layers with heat, first reported by the Frechét group11 and made technologically viable by the Krebs group,[12] using carboxylic acid ester pyrolysis/decarboxylation as thermo-cleavage for polythiophenes,[14,15] set the basis for our work. The disadvantage of this particular approach is the direct connection of the ester group to the polymer backbone which causes changes in the electronic properties of the polymers as observed for various substituted polythiophenes.[16] Another drawback is the high decarboxylation temperature (300 °C) that is necessary to yield a semiconducting polythiophene which is compatible only with very heat-resistant flexible substrates.[17]

In this paper we show that placing a spacer between the polymer backbone and the cleavable side chain helps to improve both issues. Although our spacer can universally attached to various conjugated polymers, we deliberately chose polythiophenes as the investigated model system to allow comparison to the literature. The electronic nature of the polythiophene remains unperturbed by the bond scissions before as well as after heat treatment. To lower the cleavage temperature, we introduce a new thermo-labile group which is based on unsymmetrical carbonates with one tertiary alcohol. Leaving a hydroxyl function on the polymeric backbone after thermal removal, these carbonates and their cleavage temperature can be modified by changing the structure of the solubilizing side chain. This is very important for the goal of printing, drying and pyrolysing these polymers (*poly*(3-(2-((alkoxycarbonyl)oxy)ethyl)thiophen-2,5-diyls **P3COET**) on low-cost flexible substrates such as polyethylene terephthalate (PET), as this limits the potential process temperatures to around 140 °C.

2. Results and discussion
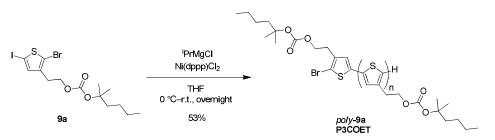
2.1. Synthesis

Scheme 1: Synthesis of hydroxyl-alkyl functionalized thiophene monomer **4** and its modification with a thermo-labile solubilizing carbonate ester.

The synthetic route to the thermo-cleavable thiophene monomer is outlined in Scheme 1. The synthesis of the thiophene building block was carried out by a bromination of commercially available 2-(3-thienyl)ethanol (**1**) with *N*-bromosuccinimide (NBS), iodination with *N*-iodosuccinimide (NIS) and hydrolysis of the resulting ester **3** to yield 2-(2-bromo-5-iodothiophen-3-yl)ethanol (**4**). The ethandiyl spacer of the 2-(2-bromo-5-iodothiophen-3-yl)ethanol (**4**) was chosen to exclude interference of the carbonate and the hydroxyl function after the cleavage, respectively, with the polymer backbone. It also allows varying the functional groups on the carbonate in a last step before polymerization.

The imidazole-*N*-carboxylic ester **7** was obtained by coupling 2-methylhexan-2-ol (**6a**) and 1,1'-carbonyldiimidazole (CDI, **5**), according to the synthetic procedure by Rannard.[18] The reason for using 2-methylhexan-2-ol (**6a**) as solubilizing alkyl chain was a compromise, given that the solubility between the uncleaved and cleaved polymer should be maximized while on the other hand producing volatile fragments.[11,12]
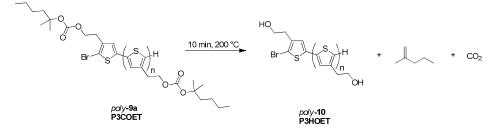
The synthesis of the final carbonate **9a** could be improved by switching the solvent from toluene (50% yield) to tetrahydrofuran (86% yield). The polymerization (**9a** to *poly*-**9a**, Scheme 2) was performed using the Kumada catalyst transfer polymerization (KCTP) reported by Yokozawa.[19] The low reaction temperature is ideal for the polymerization of thermo-labile thiophenes **9**, so that no cleavage of the thermo-labile solubilizing chains can occur.

Scheme 2: KCT Polymerization of the thermo-labile thiophene monomer **9a** to give **P3COET** *poly*-**9a**.

After precipitation from methanol and Soxhlet extraction, the new **P3COET** polymer *poly*-**9a** was characterized by size exclusion chromatography, while the regioregularity was measured by ^{1}H NMR spectroscopy. The **P3COET**s were purified and fractionated by Soxhlet extraction with different solvents (methanol followed by acetone and chloroform). The methanol fraction contained only monomers and oligomers, the acetone and chloroform fractions provided two polythiophenes: acetone fraction (39%): M_n = 15.3 kg/mol, M_w = 24.6 kg/mol, PDI = 1.6; chloroform fraction (15%): M_n = 41.0 kg/mol, M_w = 45.6 kg/mol, PDI = 1.1.

2.2.   Characterization of *poly*-9a and its pyrolysis product

Scheme 3: The decomposition reaction of **P3COET** *poly*-**9a** to **P3HOET** *poly*-**10** after heating at 200 °C for 10 minutes.
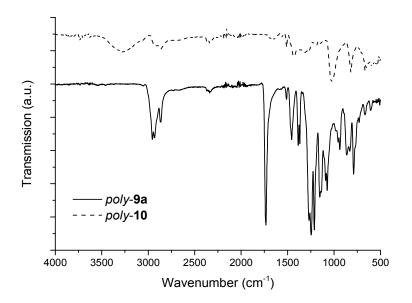
Figure 1: IR spectra of **P3COET** *poly*-**9a** (solid) and **P3HOET** *poly*-**10** (dashed).

IR spectroscopy is a very convenient analytical characterization technique to indicate whether the polymer consists of carbonates only or already has some cleaved functionalities on the backbone (i.e. alcohols). IR-spectra before (dashed) and after (solid) the cleavage clearly show the split-off of the solubilizing group (Figure 1). The carbonates in *poly*-**9a** give rise to a strong band at 1737 cm^{-1} which can be assigned to the carbonyl stretching mode. After the cleavage, the carbonyl band disappears completely and the liberated alcohol functionality (3230 cm^{-1}) of **P3HOET** *poly*-**10** (*poly*-3-(2-hydroxyethyl)thiophene-2,5-diyl) can be detected.

The relative (in-)stability of the **P3COET**s was investigated by thermogravimetric analysis (TGA) in conjunction with differential scanning calorimetry (DSC) in the temperature range up to 300 °C (Figure 2). The carrier gas leaving the furnace was analyzed by mass spectrometry and Fourier transform infrared spectroscopy (TGA-MS-FTIR, see ESI). These measurements corroborate the evaporation of 2-methyl-2-hexene and carbon dioxide from the sample starting at 180 °C reaching its maximum at 200 °C.
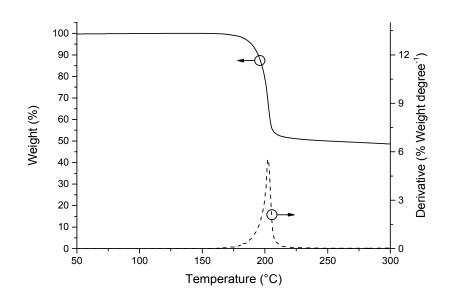
Figure 2: Thermo-gravimetric analysis of **P3COET** *poly*-**9a** in the temperature range of 50–300 °C. The data was recorded at an increasing temperature of 10 °C min^{-1} under nitrogen atmosphere. A derivative weight loss curve has been included to indicate the point with the most apparent weight loss.
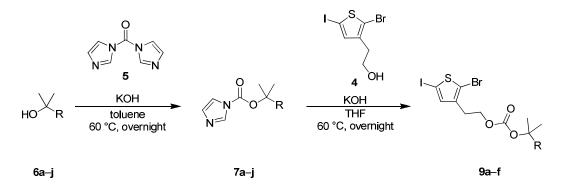
The optical and electronic properties of the carbonate-functionalized polythiophene *poly*-**9a** were investigated by UV-Vis spectroscopy and cyclic voltammetry (CV) measurements (see Supporting Information). The introduction of the carbonate with a C_2-spacer has a small effect on the UV-Vis spectra of the polythiophene. This hints to a slightly higher non-planarity of the conjugated backbone than in common poly(3-hexylthiophene) (P3HT) because of the different length and steric demand of the solubilizing alkyl chain.[3] The CV measurement (*poly*-**9a** film in acetonitrile against Fc/Fc$^+$) confirms the equal electronic properties of the polythiophene *poly*-**9a** (E_{ox} = 0.52 V) compared to P3HT.[20]

2.3. Control of cleavage temperature

To enable the use of our thermo-labile polymers on low-cost flexible substrates (like e.g. PET), their structure should be modified to reduce the cleavage temperature to around 140°C. Ab initio and experimental studies by Van Speybroeck revealed that a six-membered cyclic transition state is required to have an optimal geometry while the C_α–O bond dissociation is the rate-determining step. Stabilization of the positive charge in the C_α position affects an acceleration of the reaction rate. The last step is a β-H-elimination or *syn*-elimination.[21][22]

According to this mechanism, it is possible to tune the elimination temperature by changing the cation-stabilizing properties of the side chain. Based on this rationale, we set out to prepare derivatives changing the alkyl into an alkenyl (**6h–j**) or alkinyl (**6e–g**) side chains, which form mesomerically stabilized cations and eventually lead to conjugated double bonds after elimination. The two methyl groups or a cyclic group next to the alcohol are necessary for stabilization and simultaneously provide β-H for the pyrolysis. The corresponding alcohols were synthesized by nucleophilic addition of Grignard reagents to carboxyl functions or lithiated alkynes to acetone, cyclopentanone or cyclohexanone, respectively. All synthesized alcohols were stable and most of them could be obtained in good to excellent yields (see Supporting Information).

Scheme 4: Syntheses of the 3-(2-((alkoxycarbonyl)oxy)ethyl)thiophene monomers **9**, starting from tertiary alcohols **6**.

Table 1: Chemical structures and yields of the alcohols, carboxyl esters and carbonates prepared in this study.

Solubilizing group	Alcohol, yield	Imidazole-*N*-carboxylic ester, yield	Carbonate, yield
	6a, –[a]	**7a**, 86%	**9a**, 86%
	6b, –[a]	**7b**, 70%	**9b**, 84%
	6c, 70%	**7c**, 31%	**9c**, 91%
	6d, 45%	**7d**, 46%	**9d**, 74%
	6e, 78%	**7e**, 74%	**9e**, 90%[c]
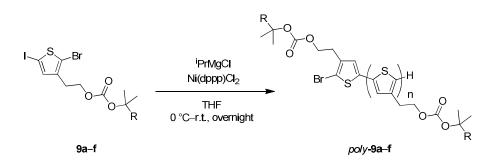
	6f, 91%	**7f**, 85%	**9f**, 80%[c]
	6g, 78%	**7g**, 17%	–
	6h, 63%	–, **8h**[b]	
	6i, 94%	–, **8i**[b]	
	6j, quant.	–, **8j**[b]	

[a]Commercially available; [b]no imidazole-*N*-carboxylic esters isolated, but the decarboxylated *N*-substituted imidazole **8h–i**; [c]triethylamine added for purification by column chromatography.

The synthesis of the imidazole-*N*-carboxylic esters **7** proved necessary for the synthesis of the asymmetric carbonates and were obtained by coupling the appropriate alcohol **6** and 1,1'-carbonyldiimidazole (CDI, **5**). Interestingly, during these reactions or their workup some imidazole-*N*-carboxylic esters already decomposed. The CDI-coupling of allylic or benzylic alcohols did not yield the imidazole-*N*-carboxylic esters but the decarboxylated *N*-substituted imidazoles (**8h–j**, see Supporting Information). This was a first hint that some imidazole-*N*-carboxylic esters and the corresponding carbonates were not stable enough to synthesize a polymer. The carbonate monomers **9** finally were obtained by reacting the imidazole-*N*-carboxylic esters **7** with 2-(2-bromo-5-iodothiophen-3-yl)ethanol (**4**). For some of the monomers (**9e** and **9f**), triethylamine had to be added to the eluent during purification by column chromatography, the silica gel otherwise being too acidic for the carbonate groups. The use of acidic additives to lower the cleaving temperature has already been shown by the Krebs group.[23] The yields of the respective imidazole-*N*-carboxylic ester syntheses allow a good forecast for the stability of the resulting carbonates **9**. We observed that imidazole-*N*-carboxylic ester **7g** with a cyclopentyl and alkinyl side chain (entry 7) was difficult to isolate and that the carbonate **9g** could not be obtained. The cyclopentyl group resulted in less stable compounds than the cyclohexyl.

Scheme 5: KCT Polymerization of thermo-labile thiophene monomers **9a–f** to obtain a series of **P3COET**s (cf. Table 2).

With this set of monomers, the corresponding polymers (Table 2) were prepared by KCTP.[19] The low reaction temperature of this reaction proves ideal for the polymerization of the monomers **9**, since it prohibits the cleavage of the thermo-labile solubilizing chains during polymerization.

Table 2: Chemical structures, yields and properties of **P3COET**s *poly*-**9a–f** obtained by KCT polymerization of **9a–f.**

	Product	**Yield** [%][a]	**M_n** [kg mol^{-1}][e]	**M_w** [kg mol^{-1}][e]	**PDI**	**Cleavage temperature**[f] [°C]
poly-**9a**		39[b] 15[c]	15.3 41.0	24.6 45.6	1.61 1.11	192
poly-**9b**		25[c]	18.4	22.9	1.25	198
poly-**9c**		5[c]	22.0	27.5	1.24	140
poly-**9d**		3[b] –[d]	4.3	4.8	1.11	168

poly-9e		20^c	8.2	10.9	1.32	174
poly-9f		23^b $\_^d$	17.9	31.7	1.77	178

[a]After Soxhlet extraction: [b]acetone-soluble; [c]chloroform-soluble; [d]non-soluble fraction in chloroform obtained after cleavage; [e]determined by SEC with polystyrene standards in chloroform; [f]temperature at 5%-weight loss measured by thermo-gravimetric analysis (at 10 °C min^{-1}).

Table 2 is a compilation of all synthesized **P3COET**s poly-**9a–f**. Obviously, the yields correlate with the cleavage temperature of the thermo-labile solubilizing chains and results from the purification method. **P3COET**s with lower cleavage temperature like poly-**9c–f** (Table 2) partially cleave during the synthesis or the purification by Soxhlet extraction because of the high temperature and the slight acidic behavior of chloroform.[23] In this case, formation of insoluble **P3HOET** poly-**10** in the Soxhlet thimble could be observed, but also the soluble polymers poly-**9c**+**d** already exhibit a small hydroxyl-band in their IR spectra. The other **P3COET**s show no hydroxyl vibrations in the IR which is in line with a higher cleavage temperature. The molecular weights (M_w) of the polymers are in the range of 4.8 kg mol^{-1} to 45.6 kg mol^{-1} and are not linked to the yields or the (in-)stability (entry 3). The dispersity (PDI) of the polymers is low. Figure 3 shows the thermal behavior of the **P3COET**s poly-**9a–f** as normalized TGA curves in the temperature range of 100–250 °C. The range of the thermal cleavage is between 140 °C (poly-**9c**, entry 3) and 198 °C (poly-**9b**, entry 2). The polymers with cyclopentyl groups (poly-**9c** and poly-**9d**; entry 3+4) are less stable than the polymers with alkynyl groups (poly-**9e** and poly-**9f**; entry 5+6).The poly-**9b** with a cyclohexyl group (entry 2) exhibits the highest cleavage temperature. The difference in the normalized TGA curve shapes depends on the boiling point of the alkene generated during the pyrolysis.
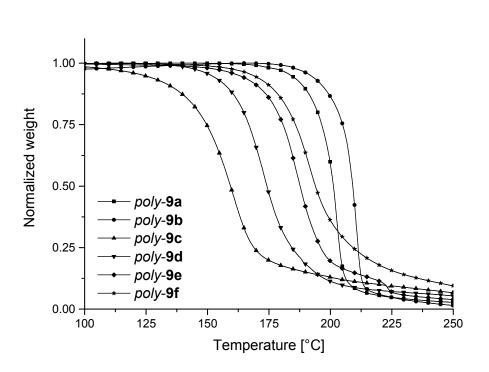
Figure 3: Normalized TGA curves of the **P3COET**s *poly*-**9a–f**. The data was recorded at an increasing temperature of 10 °C min^{-1} under nitrogen atmosphere.

2.4.   Thin film structural analysis

The control over the surface arrangement of conjugated polymers is essential for their application in electronic devices. Generally, transistors require an edge-on polymer arrangement favoring the charge carrier transport parallel to the dielectric surface.[24] On the other hand, the efficiency of solar cells can be improved by a face-on assembly when the π-stacking direction is oriented perpendicular to the substrate and thus in the direction of the charge carrier transport. Different approaches related to polymer design and processing have been reported to control the surface organization of polymers. For instance, the morphology of P3HT thin-films can be tuned by substrate treatment[25] and the solvents used for thin-film fabrication.[26] The annealing of a polymer at its melting temperature can also change the surface organization as in the case of poly-naphthalene-bithiophene from face-on, obtained after spin-coating, to edge-on.[27] Concerning the polymer design, the organization of P3HT can be controlled by its regioregularity.[28] The aggregation in solution also plays an important role and is affected by the polymer interactions. Polymers with bulky substituents reducing aggregation assemble on the surface face-on, while macromolecules

with strong interactions and subsequent aggregation in solution are arranged edge-on.[29] In bulk-heterojunction structures for solar cells, PCBM acts like a plasticizer for the conjugated polymers and can induce reorganization of the polymer mostly to face-on, thus enhancing the device efficiency.[30]

2.4.1. Neat P3COET polymer films

In order to identify differences in polymer organization before and after thermal cleavage of solution deposited thin films of **P3COET** poly-**9a**, grazing incidence wide-angle X-ray scattering (GIWAXS) measurements were performed. Since poly-**9a** can be applied in at least two different types of devices, field-effect transistors and organic solar cells, two kinds of samples were investigated (pure **P3COET** and its blend with an acceptor). In the first case, drop-cast or spin-coated neat poly-**9a** samples were fabricated according to the procedures used for the transistor fabrication (see Supporting Information).
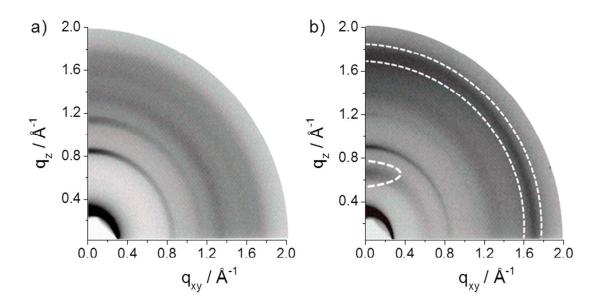
Figure 4: GIWAXS patterns of drop-cast films of poly-**9a** after annealing (a) at 100 $^{\circ}$C and (b) at 200 $^{\circ}$C. Meridional reflection related to the new interlayer and π-stacking peak are indicated by dashed circles.

Large variation in packing for poly-**9a** drop-cast films before and after annealing at 200 °C is evident from the GIWAXS patterns presented in Figure 4. Both patterns reveal quite isotropic reflections indicating a rather random distribution of the crystallites towards the surface. This is not surprising, since the drop-cast films are relatively thick with no preferential growth direction of the polymers. Nevertheless, the maximum intensity of the h00 reflection on the meridional plane implies certain preference of the polymer orientation

on the surface. This reflection is assigned to an interlayer distance of 2.20 nm of layers arranged parallel to the substrate with quasi edge-on polymer backbones. In comparison to regioregular P3HT (d = 1.57 nm),[31] the larger layer spacing obtained for *poly*-**9a** is caused by the attached thermally sensitive alkyl chains. In addition, the substituents influence the interaction between polymers. The lack of a corresponding π-stacking peak of poly-**9a** before annealing suggests highly disordered polymer packing within the layer structures (Figure 4a). The GIWAXS pattern in Figure 4b is obtained for *poly*-**9a** after thermal cleavage of the substituents (i.e. **P3HOET** *poly*-**10**). The interlayer distance observed for the unannealed film is slightly reduced from 2.20 nm to 2.15 nm. In addition, a new reflection on the meridional plane is observed for $q_z = 0.67$ Å^{-1} and $q_{xy} = 0$ Å^{-1} related to a d-spacing of 0.93 nm. This value is in agreement with the diameter of the polymer after thermal cleavage. The appearance of this reflection indicates the co-existence of two structures with independent interlayer spacings of 2.15 nm and 0.93 nm. Most probably the thick drop-cast film undergoes only partly the cleavage reaction leading to the formation of both phases. The film heterogeneity is also the reason for the low level of the charge carrier mobility in field-effect transistors of 10^{-5} cm²/Vs before and after thermo-cleavage (see Supporting Information). To ensure more homogenously thermo-cleavage in the thin spin-coated samples, the films were treated at lower temperatures for significantly longer annealing times.This process allows thermo-cleavage through the entire film leading solely to an interlayer distance of 0.93 nm (Figure S2). In general, the crystallinity of the spin-coated films is lower in comparison to drop-casting due to longer evaporation time of the solvent and thus extended kinetics of the structure growth in the latter case. A further interesting change in the drop-cast film after the cleavage of the substituents is the increased packing order of the polymers as evident from the additional π-stacking reflection in the wide-angle scattering range related to a distance of 0.37 nm. It can be assumed that the steric demand of the substituent is reduced after thermo-cleavage allowing a stronger interaction between the conjugated **P3HOET** backbones.

2.4.2. Polymer:PCBM films

In order to integrate *poly*-**9a** into the absorber layers of bulk-heterojunction organic photovoltaic devices, we studied the thin-film formation of a polymer:fullerene blend upon deposition from solution. Therefore, we dissolved *poly*-**9a** and [6,6]-phenyl C$_{61}$-butyric acid

methyl ester (PCBM) 1:0.5 (wt:wt) in 1,2-dichlorobenzene and spin cast the layer from the respective solution. We assessed the bulk-heterojunction homogeneity by atomic force microscopy (AFM). The thin-film topography of films that were annealed at 150 °C, is depicted in Figure 5. The layers exhibited a root-mean-square roughness $r_q \approx 0.36$ nm and did not exhibit any pinholes. Upon annealing at 200 °C and hence above the cleavage temperature, the surface texture became rougher ($r_q \approx 4.49$ nm) and, besides some larger aggregates, exhibited grains with a typical size of 10 nm that were randomly distributed all over the layer surface. Most importantly, upon annealing, these layers were almost insoluble in the process solvent, i.e. 1,2-dichlorobenzene.
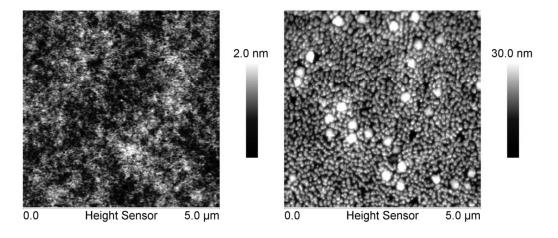
Figure 5: Surface texture of *poly*-**9a**:PCBM (1:0.5 wt/wt) films (a) after annealing at 150 °C and (b) after annealing at 200 °C and side chain cleavage.

When investigated by X-ray diffraction, the effect of the thermo-cleavage on the polymer packing in *poly*-**9a** thin films is even more evident in the bulk-heterojunction structure. Figure 6 depicts the GIWAXS patterns obtained for thin spin-coated *poly*-**9a**:PCBM layers on *poly*(3,4-ethylenedioxythiophene):polystyrenesulfonate (PEDOT:PSS) before and after thermo-cleavage at 200 °C. The film before annealing is quite disordered as only one single peak on the meridional plane at $q_z = 0.285$ Å^{-1} and $q_{xy} = 0$ Å^{-1} is observed. This reflection is assigned to the *poly*-**9a** interlayer distance of 2.20 nm which is in agreement with the measurement of the drop-cast sample. Identically to the drop-cast film before thermal cleavage, no π-stacking reflection can be discerned for the spin-coated *poly*-**9a**:PCBM blend before annealing at 200 °C. As reported in literature, PCBM does not show any crystalline organization up to an annealing temperature of 142 °C.[32] Annealing above the pyrolysis temperature (200 °C) drastically changes the GIWAXS pattern for the bulk-

heterojunction structure. The main difference in the obtained pattern is the lack of the small-angle meridional reflection previously assigned to the layer arrangement. Interestingly, in the small-angle equatorial plane a new reflection at q_{xy} = 0.63 Å^{-1} q_z = 0 Å^{-1} appears corresponding to a d-spacing of 0.99 nm. This value is in agreement with the changes observed in the drop-cast and the spin-coated *poly*-**9a** film after thermal cleavage (Figure S2). However, in the bulk-heterojunction blend, the interlayer reflection moves from the meridional to equatorial plane suggesting a change of the backbone organization from edge-on to face-on. Furthermore, the face-on organization after thermo-cleavage is confirmed by the appearance of the π-stacking reflection (0.38 nm) in the wide-angle meridional plane.

In this work, the rearrangement of *poly*-**9a** occurs after annealing and thermal cleavage of the substituents. The reorganization is attributed to the film plasticization by PCBM, increasing the mobility of the polymer chains during thermal cleavage.[30] During this annealing step, PCBM crystalizes as evident from the spot-like reflections observed in the off-meridional range of the pattern (Figure 6b) which has also been observed in the AFM measurements.[32] Consequently, the intralayer order increases, while the interlayer distance decreases. The higher order within the layers enhances the charge carrier transport in π-stacking direction which, after the reorganization, coincides with the direction of the applied electric field in solar cells. Additionally, the shorter interlayer periodicity and less dense isolating alkyl mantle facilitates transport between layers. This increases the dimensionality of the charge carrier transport, allowing an easier by-passing of structural defects such as trapping sites.
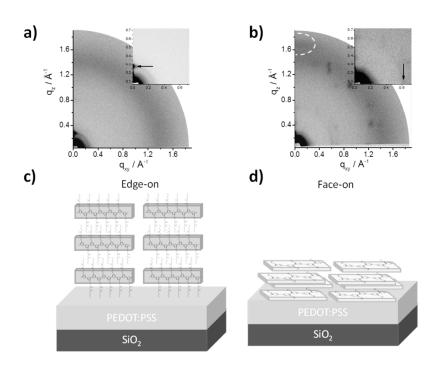
Figure 6: GIWAXS patterns of *poly*-**9a**:PCBM thin films on PEDOT:PSS (a) before and (b) after thermo-cleavage at 200 °C (meridional π-stacking reflection is indicated by the dashed circle). Insets show the small-range scattering range with the interlayer reflection indicated by an arrow. Schematic illustrations of the *poly*-**9a** surface organization obtained after fabrication with (c) edge-on and (d) face-on arrangement after thermal annealing at 200 °C (due to simplicity, PCBM is omitted).

2.5. Bulk-heterojunction solar cells

The good film quality enabled the *poly*-**9a**:PCBM (1:0.5 wt/wt) layer integration into organic photovoltaic devices with an ITO/PEDOT:PSS/poly-**9a**:PCBM/Ca/Al device architecture. The solar cell with the absorber layer that was annealed at 150 °C, *i.e.*, below the cleavage temperature, exhibits very poor performance, particularly due to a very low photo current, as depicted in Figure 7a. Upon annealing at 200 °C and side chain cleavage, the photo current increases significantly to 4.2 mA/cm^2 and hence the device power conversion efficiency improves to 1.2%. This observation may partly be attributed to the low PCBM load in the bulk-heterojunction which commonly depends on the degree of intercalation of polymer and fullerene. For optimized P3HT:PCBM solar cells, the blend ratio is on the order of 1:1. Here, the improvement of the device performance upon annealing at 200 °C and the removal of the side chains leads to a reduced intercalation. The reduced intercalation in turn enables better device efficiencies with reduced PCBM load. This assumption is supported by the concentration dependent J-V measurements that are depicted in Figure 7b., where we

varied the *poly*-**9a**:PCBM blend ratio from 1:1.25 to 1:0.5. We clearly observe an enhancement of the photo current towards lower PCBM concentrations. Hence, the removal of the bulky side chains does not only provide a change in layer solubility but also reduces the required amount of fullerenes in the bulk-heterojunction.
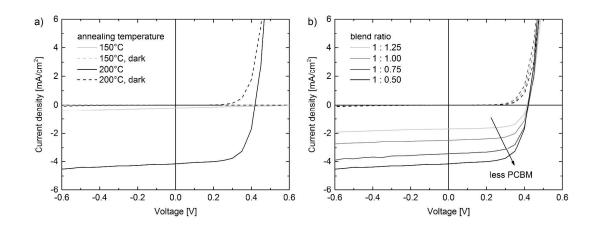
Figure 7: (a) Typical J-V curves of *poly*-**9a**:PCBM (1:0.5 wt/wt) solar cells comprising photo-active layers that were annealed below (gray) and above the cleavage temperature(black), i.e., 150 °C and 200 °C, respectively. (b) PCBM concentration dependent J-V measurements of devices that were annealed at 200 °C. The lower the PCBM load the better is the device performance (dashed lines: dark curve ~~measurement without illumination~~).

Table1: Solar Cell Parameters for the non-treated solar cell and the thermally treated cells with varying polymer:fullerene ratio.

polymer:fullerene blend ratio	annealing temperature	J_{SC} [mA/cm²]	V_{OC} [V]	FF [%]	μ_{eff} [%]
1:1.25	200°C	1.7	0.41	68	0.5
1:1.0	200°C	2.5	0.42	68	0.7
1:0.75	200°C	3.4	0.42	69	1.0
1:0.5	200°C	4.2	0.42	66	1.2
1:0.5	150°C	0.2	0.68	24	0.03

3. Conclusion

We synthesized a series of novel carbonate-functionalized thiophene monomers and regioregular polythiophenes **P3COET**s of variable pyrolysis temperature. By tuning the stabilization of the cleavage fragments, we control the onset of the pyrolysis down to a temperature region which is compatible with low-cost polymeric substrates like PET. TGA measurements in combination with IR spectroscopic studies verify the completeness and the selectivity of the cleavage to the corresponding **P3HOET**.

Based on untreated P3COETs, lateral charge transport was observed in TFTs. After the pyrolysis, however, no working TFT could be obtained. On the other hand, the efficiency of the solar cells was dramatically improved upon pyrolysis. This intriguing observation could be rationalized based on GIWAXS measurements in thin films of either pure **P3COET**, the pyrolysed **P3HOET** and the respective blends with PCBM on device-relevant substrates. These polythiophenes exhibit different preferential orientation with respect to the surface from edge-on before and face-on after cleavage, explaining the observed swap in device performance.

Due to the mass-loss during cleavage, the relative amount of PCBM necessary to obtain solar cells with maximum efficiency is drastically reduced compared to non-cleavable polythiophenes like P3HT.

The compounds presented in this study show the potential of thermo-cleavable solubilizing side chains with controllable cleavage temperature. The moderate process temperature enables device fabrication on low-cost substrates. The reduced diffusivity of the polymers after cleavage enables the generation of morphologically more robust thin films which may lead to long-term stability of the morphology. Cleaving off the side chains and hence significantly reducing the material solubility makes this concept interesting for future multi-layer organic optoelectronic devices, in particular when transferred to high-performance amorphous polymers.

4. Acknowledgments

5. Supporting Information

1
2
3   Supporting Information (Experimental and analytical data on all prepared compounds, thin
4
5   film transistor and solar cell fabrication details and characterization data) is available from
6
7   http://pubs.acs.org/ or from the authors.
8
9
10
11
12   [1] Pron, A.; Gawrys, P.; Zagorska, M.; Djuradoa, D.; Demadrillea, R., *Chem. Soc. Rev.* **2010,** 39, 2577–2632.
13   [2] Mei, J.; Bao, Z., *Chem. Mater.* **2014,** 26, 604–615.
14   [3] Hotta, S.; Rughooputh, S. D. D. V.; Heeger, A. J.; Wudl, F., *Macromolecules* **1987,** 20, 212–215.
15   [4] Mei, J.; Kim do, H.; Ayzner, A. L.; Toney, M.F.; Bao, Z., *J. Am. Chem. Soc.* **2011,** 133, 20130–20133.
16   [5] Lei, T.; Dou, J.-H.; Pei, J., *Adv. Mater.* **2012,** 24, 6457-6461.
17   [6] Lei, T.; Wang, J.-Y.; Pei, J., *Chem. Mater.* **2014,** 26, 594–603.
18   [7] Li, W.; Wang, Q.; Ji Cui, H. C.; Shaheen, S. E.; Jabbour, G. E.; Anderson, J.; Lee, P.; Kippelen, B.; Peyghambarian, N.; Armstrong, N. R.; Marks, T. J., *Adv. Mater.* **1999,** 11, 730–734.
20   [8] Bayerl, M. S.; Braig, T.; Nuyken, O.; Müller, D. C.; Groß, M.; Meerholz, K., *Macromol. Rapid Commun.* **1999,** 20, 224–228.
22   [9] Huang, F.; Wu, H.; Cao, Y., *Chem. Soc. Rev.* **2010,** 39, 2500–2521.
23   [10] Sax, S.; Rugen-Penkalla, N.; Neuhold, A.; Schuh, S.; Zojer, E.; List, E. J. W.; Müllen, K., *Adv. Mater.* **2010,** 22, 2087–2091.
25   [11] Liu, J.; Kadnikova, E. N.; Liu, Y.; McGehee, M. D.; Fréchet, J. M. J., *J. Am. Chem. Soc.* **2004,** 126, 9486–9487.
26   [12] Bjerring, M.; Nielsen, J. S.; Nielsen, N. C.; Krebs, F. C., *Macromolecules* **2007,** 40, 6012–6013.
27   [13] Yu, J.; Holdcroft, S., *Macromolecules* **2000,** 33, 5073–5079.
28   [14] Petersen, M. H.; Gevorgyan, S. A.; Krebs, F. C., *Macromolecules* **2008,** 41, 8986–8994.
29   [15] Hagemann, O.; Bjerring, M.; Nielsen, N. C.; Krebs, F. C., *Sol. Energy Mater. Sol. Cells* **2008,** 92, 1327–1335.
30   [16] Krebs, F. C.; Spanggaard, H., *Chem. Mater.* **2005,** 17, 5235–5237.
31   [17] Krebs, F. C.; Norrman, K., *ACS Appl. Mater. Interfaces* **2010,** 2, 877–887.
32   [18] Rannard, S. P.; Davis, N. J., *Org. Lett.* **1999,** 1, 933–936.
33   [19] Miyakoshi, R.; Yokoyama, A.; Yokozawa, T., *J. Am. Chem. Soc.* **2005,** 127, 17542–17547.
34   [20] Xin, H.; Guo, X.; Kim, F. S.; Ren, G.; Watson, M. D.; Jenekhe, S. A., *J. Mater. Chem.* **2009,** 19, 5303–5310.
35   [21] Speybroeck, V. V.; Martelé, Y.; Waroquier, M.; Schacht, E., *J. Am. Chem. Soc.* **2001,** 123, 10650–10657.
36   [22] Speybroeck, V. V.; Martelé, Y.; Schacht, E.; Waroquier, M., *J. Phys. Chem. A* **2002,** 106, 12370–12375.
37   [23] Søndergaard, R. R.; Norrman, K.; Krebs, F. C., *J. Polym. Sci., Part A: Polym. Chem.* **2012,** 50, 1127–1132.
38   [24] Guo, X.; Puniredd, S. R.; Baumgarten, M.; Pisula, W.; Müllen, K., *Adv. Mater.* **2013,** 25, 5467–5472.
39   [25] Joshi, S.; Pingel, P.; Grigorian, S.; Panzner, T.; Pietsch, U.; Neher, D.; Forster, M.; Scherf, U., *Macromolecules* **2009,** 42, 4651–4660.
41   [26] Kline, R. J.; McGehee, M. D.; Kadnikova, E. N.; Liu, J.; Fréchet, J. M. J.; Toney, M. F., *Macromolecules* **2005,** 38, 3312–3319.
43   [27] Rivnay, J.; Steyrleuthner, R.; Jimison, L. H.; Casadei, A.; Chen, Z.; Toney, M. F.; Facchetti, A.; Neher, D.; Salleo, A., *Macromolecules* **2011,** 44, 5246–5255.
45   [28] Sirringhaus, H.; Brown, P. J.; Friend, R. H.; Nielsen, M. M.; Bechgaard, K.; Langeveld-Voss, B. M. W.; Spiering, A. J. H.; Janssen, R. A. J.; Meijer, E. W.; Herwig, P.; de Leeuw, D. M., *Nature* **1999,** 401, (6754), 685–688.
47   [29] Chen, M. S.; Lee, O. P.; Niskala, J. R.; Yiu, A. T.; Tassone, C. J.; Schmidt, K.; Beaujuge, P. M.; Onishi, S. S.; Toney, M. F.; Zettl, A.; Fréchet, J. M. J., *J. Am. Chem. Soc.* **2013,** 135, 19229–19236.
49   [30] Osaka, I.; Saito, M.; Mori, H.; Koganezawa, T.; Takimiya, K., *Adv. Mater.* **2012,** 24, 425–430.
50   [31] Shao, M.; Keum, J.; Chen, J.; He, Y.; Chen, W.; Browning, J. F.; Jakowski, J.; Sumpter, B. G.; Ivanov, I. N.; Ma, Y.-Z.; Rouleau, C. M.; Smith, S. C.; Geohegan, D. B.; Hong, K.; Xiao, K., *Nat. Commun.* **2014,** 5, 1–11.
52   [32] Verploegen, E.; Mondal, R.; Bettinger, C. J.; Sok, S.; Toney, M. F.; Bao, Z., *Adv. Funct. Mater.* **2010,** 20, 3519–3529.

Supporting Information

Tertiary Carbonate Side Chains: Easily Tuneable Thermo-Labile Breaking Points for Controlling the Solubility of Conjugated Polymers

Marius Kuhn,[a)d)] Jens Ludwig,[b)] Tomasz Marszalek,[c)] Torben Adermann,[a)d)] Wojciech Pisula,[c)] Klaus Müllen,[c)d)] Alexander Colsmann,[b)] Manuel Hamburger[a)d)]*

a) Institute of Organic Chemistry, Heidelberg University, Im Neuenheimer Feld 270, 69120 Heidelberg, Germany

b) Light Technology Institute, Karlsruhe Institute of Technology (KIT), Engesserstr. 13, 76131 Karlsruhe, Germany

c) Max Planck Institute for Polymer Research, Ackermannweg 10, 55128 Mainz, Germany

d) InnovationLab GmbH, Speyerer Str. 4, 69115 Heidelberg, Germany

S1. Experimental.

General Remarks

All reactions requiring exclusion of oxygen and moisture were carried out in dry glassware under a dry and oxygen free argon or nitrogen atmosphere. For spectroscopic and analytic characterizations the following devices were available:

Analytical Thin Layer Chromatography (TLC) was performed on Macherey-Nagel Polygram® SIL G/UV$_{254}$ precoated sheets. Components were visualized by observation under UV irradiation (254 nm and 365 nm) or with molybdophosphoric acid solution in ethanol.

Flash Column Chromatography was carried out on silica gel (0.032 mm-0.062 mm), purchased from Macherey, Nagel & Co.

DSC and **TGA** measurements were carried out on a Mettler-Toledo TGA/DSC1 instrument with a TGA/DSC-Sensor 1100 equipped with a MX1 balance (Mettler-Toledo) and a GC100 gas control box for nitrogen supply.

^{1}H NMR and **^{13}C-NMR** spectra were recorded at room temperature on Bruker Avance DRX 300 (300 MHz) and Bruker Avance III 300 (300 MHz). Chemical shifts (δ) are reported in parts per million (ppm) relative to residual undeuterated solvent peak. The following abbreviations are used to indicate the signal multiplicity: s (singlet), d (doublet), t (triplet), q (quartet), m (multiplet), dd (doublet of doublet), bs (broad singlet). All NMR spectra were integrated and processed using TopSpin 3.0.

High Resolution Mass Spectra (HR-MS) were determined at the Organisch-Chemisches Institut of the University of Heidelberg under the direction of Dr. J. Gross. All methods were recorded on a Vakuum Generators ZAB-2F (EI$^+$), Finnigan MAT TSQ 700 (ESI$^+$) or JEOL JMS-700 (FAB$^+$) spectrometer.

Infrared (IR) Spectra were recorded on a Jasco FT/IR-4100 spectrometer as neat oil or powder.

Absorption Spectra were carried out on a Jasco UV-VIS V-660 or Jasco UV-VIS V-670 in solution or in solid state *via* a spin-coated glass-slide.

Emission Spectra were recorded on a Jasco FP-6500 in solution or in solid state *via* a spin-coated glass-slide.

Cyclic Voltammetry was performed with a VERSASTAT3-200 potentiostat (Princeton Applied Research) using a glassy carbon, gold or platin working electrode, a 0.1 mol/l Bu$_4$N$^+$ ClO$_4^-$ or Bu$_4$N$^+$ PF$_6^-$ solution in methylene chloride or THF as solvent and ferrocene/ferrocenium as reference redox system and internal or external standard.
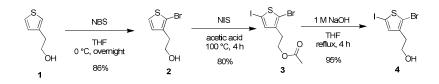
Gel Permeation Chromatography was performed with Jasco intelligent RI- and UV/Vis-detectors (RI-2031Plus, UV-2075Plus). Number- (M_n) and weight average (M_w) molecular weights and polydispersities (PDI) were determined by GPC versus polystyrene standards. Measurements were carried out at room temperature in chloroform (flow rate 1 mL/min) with PSS-SDV columns (8.0 mm x 30.0 mm, 5 µm particles, 10^2-, 10^3- and 10^5- Å pore size). All GPC traces were analyzed and processed by PSS WinGPC Unity Build 9350.

Atomic Force Microscopy (AFM) measurements were performed on a Bruker Dimension ICON under inert conditions. Scan Asyst silicon nitride cantilevers from Bruker (70 kHz, 0.4 N/m) were used as sensors.

IUPAC names and atom numberings of the compounds described in the experimental section were determined with the program ACD/ChemScetch 2012 of Advanced Chemistry Development Inc.

Solvents were purchased from the store of the Theoretikum or chemical store at the Organisch-Chemisches Institut of the University of Heidelberg and if necessary distilled prior use. All of the other absolute solvents were dried by a MB SPS-800 using drying columns.

Chemicals were either purchased from the chemical store at the Organisch-Chemisches Institut of the University of Heidelberg or from commercial laboratory suppliers. Reagents were used without further purification unless otherwise noted.

Synthesis.

Scheme S1: Synthesis of 2-(2-Bromo-5-iodothiophen-3-yl)ethanol (4).

2-(2-Bromothiophen-3-yl)ethanol (**2**): N-bromosuccinimide (11.2 g, 62.5 mmol, 1.00 eq.) was added portionwise at 0 °C to a solution of 2-(thiophen-3-yl)ethanol (**1**) (8.02 g, 62.5 mmol, 1.00 eq.) in tetrahydrofurane (200 mL), and the mixture was stirred at 0 °C overnight. The product was extracted with water and chloroform, washed with sodium hydrogen carbonate solution, and dried over anhydrous $MgSO_4$. The crude product was further purified by column chromatography using petroleum ether/ethyl acetat 2:1 as the eluent to give a yellow oil (11.1 g, 86%). – ^{1}H-NMR (300 MHz, $CDCl_3$): δ = 7.26 (d, ^3J = 5.6 Hz, 1 H, H_{ar}), 6.90 (d, ^3J = 5.6 Hz, 1 H, H_{ar}), 3.86 (t, ^3J = 6.6 Hz, 2 H, CH_2-OH), 2.89 (t, ^3J = 6.6 Hz, 2 H, C_{ar}-CH_2), 1.75 (s, 1 H, OH). – ^{13}C-NMR (75 MHz, $CDCl_3$): δ = 138.1 (C_{ar}-CH_2), 128.7 (C_{ar}), 125.8 (C_{ar}),

110.5 (C_{ar}-Br), 62.2 (CH_2-OH), 32.9 (C_{ar}-CH_2). − MS (EI), m/z (%): 208/206 (52/51) [M⁺], 177/175 (100/91) [(C_5H_4BrS)⁺], 97 (38). − HRMS (C_6H_7BrOS): ber. 205.9401, gef. 205.9402.

2-(2-Bromo-5-iodothiophen-3-yl)ethyl acetate (3): 2-(2-Bromothiophen-3-yl)ethanol **(2)** (9.11 g, 44.0 mmol, 1.00 eq.) was dissolved in acetic acid (50 mL). After addition of *N*-iodosuccinimide (10.4 g, 46.2 mmol, 1.05 eq.) the resulting suspension was stirred at 100 °C for 4 h. Then the mixture was poured into water and the organic layer was taken off while the water phase was extracted with dichloromethane. The combined organic phases were washed with 1 M sodium hydroxide solution, 10% sodium thiosulfate solution water, brine and were dried over MgSO₄. The crude product was further purified by column chromatography using petroleum ether/ethyl acetat 3:1 as the eluent to give a orange oil (15.4 g, 93%). − ¹H-NMR (300 MHz, CDCl₃): δ = 7.01 (s, 1 H, H_{ar}), 4.20 (t, ³J = 6.9 Hz, 2 H, CH_2-O), 2.88 (t, ³J = 6.9 Hz, 2 H, C_{ar}-CH_2) 2.05 (s, 3 H, CH_3). − ¹³C-NMR (75 MHz, CDCl₃): δ = 171.0 (*C*=O), 140.0 (C_{ar}-CH_2), 138.1 (C_{ar}), 113.7 (C_{ar}-Br), 71.7 (C_{ar}-I), 63.2 (CH_2-O), 28.8 (C_{ar}-CH_2), 21.2 (CH_3). − MS (EI), m/z (%): 376/374 (15/15) [M⁺], 316/314 (100/100) [(C_6H_4BrIS)⁺], 190/188 (8/9) [(C_6H_5BrS)⁺]. − HRMS ($C_8H_8BrIO_2S$): ber. 373.8473, gef. 373.8463.

2-(2-Bromo-5-iodothiophen-3-yl)ethanol (4): 2-(2-Bromo-5-iodothiophen-3-yl)ethyl acetate **(3)** (17.1 g, 45.7 mmol, 1.00 eq.) was dissolved into 350 mL of THF and 200 mL of 1 M sodium hydroxide solution and stirred at 70 °C for 4 h. The mixture was diluted with toluene and washed several times with water, dried over MgSO₄, filtered and concentrated to give a colorless solid (14.9 g, 98%). − ¹H-NMR (300 MHz, CDCl₃): δ = 7.06 (s, 1 H, H_{ar}), 3.82 (t, ³J = 6.4 Hz, 2 H, CH_2-OH), 2.82 (t, ³J = 6.4 Hz, 2 H, C_{ar}-CH_2), 1.44 (s, 1 H, OH). − ¹³C-NMR (75 MHz, CDCl₃): δ = 140.5 (C_{ar}-CH_2), 138.4 (C_{ar}), 113.4 (C_{ar}-Br), 71.8 (C_{ar}-I), 62.0 (CH_2-OH), 32.7 (C_{ar}-CH_2). − MS (EI), m/z (%): 334/332 (91/94) [M⁺], 303/301 (100/99) [(C_5H_3BrIS)⁺]. − HRMS (C_6H_6BrIOS): ber. 331.8367, gef. 331.8363.

Table S1: Overview of the tertiary alcohols used in this study.

Entry		Alcohol	Preparation method	Yield [%]
1	6a	HO⟨structure⟩	_[a]	_

2	6b		_a	–
3	6c		A	70
4	6d		A	45
5	6e		B	78
6	6f		B	91
7	6g		B	78
8	6h		A	63
9	6i		A	94
10	6j		A	100

[a]Commercially available.

1-Butylcyclopentanol (**6c**): 1.6 M butyllithium in hexane (31.3 mL, 3.20 g, 50.0 mmol, 1.00 eq.) was added to a solution of cyclopentanone (4.21 g, 50.0 mmol, 1.00 eq.) in the presence of 0.6 M lanthanum chloride bis(lithium chloride) complex (40.0 mL, 4.13 g, 12.5 mmol, 0.25 eq.) in tetrahydrofurane at −78 °C. The reaction mixture was left to warm up to room temperature. After 18 h, ammonium chloride solution (2 mL) was added and the aqueous layer was extracted with diethyl ether. The combined extracts were dried over Na_2SO_4 and concentrated. The crude product was further purified by column chromatography using petroleum ether/ethyl acetat 10:1 as the eluent to give a yellow liquid (5.46 g, 70%). − ^{1}H-NMR (300 MHz, CDCl₃): δ = 1.74–1.86 (m, 3 H, OH + CH_2), 1.52–1.66 (m, 8 H, 4 × CH_2), 1.26–1.43 (m, 4 H, 2 × CH_2), 0.91 (t, ^3J = 7.0 Hz, 3 H, CH_3). − ^{13}C-NMR (75 MHz, CDCl₃): δ = 82.7 (C_q-OH), 41.4 (CH_2), 39.8 (2 × CH_2), 27.1 (CH_2), 24.0 (2 × CH_2), 23.5 (CH_2), 14.3 (CH_3). − FTIR: ṽ = 3376, 2954, 2871, 1696, 1634, 988 cm^{-1}. − MS (EI), m/z (%): 142 (6) [M$^+$], 113 (57) [(C₇H₁₃O)$^+$], 110 (23) [(C₇H₁₃O)$^+$], 85 (100) [(C₅H₉O)$^+$], 85 (100) [(C₅H₉O)$^+$], 58 (29). − HRMS (C₉H₁₈O): ber. 142.1358, gef. 142.1345.

1
2
3
4
5
6
7
8
9
10
11
12
13
14
15
16
17
18
19
20
21
22
23
24
25
26
27
28
29
30
31
32
33
34
35
36
37
38
39
40
41
42
43
44
45
46
47
48
49
50
51
52
53
54
55
56
57
58
59
60

1-Pentylcyclopentanol (**6d**): Pentylmagnesium bromide (38.6 g, 200 mmol, 1.10 eq.) in diethyl ether (100 mL) was added slowly to a solution, cooled to 0 °C, of cyclopentanone (15.3 g, 182 mmol, 1.00 eq.) in diethyl ether (200 mL). The reaction mixture was stirred at room temperature overnight. The mixture was cooled to 0 °C again, quenched with ammonium sulfate solution (200 mL), washed with water and brine and dried over $MgSO_4$, filtered and concentrated. The crude product was further purified by column chromatography using petroleum ether/ethyl acetat 10:1 as the eluent to give a yellow liquid (12.7 g, 45%). – ^{1}H-NMR (300 MHz, CDCl$_3$): δ = 1.69–1.85 (m, 3 H, O*H* + C*H$_2$*), 1.53–1.64 (m, 8 H, 4 × C*H$_2$*), 1.23–1.43 (m, 6 H, 3 × C*H$_2$*), 0.88 (t, ^3J = 6.7 Hz, 3 H, C*H$_3$*). – ^{13}C-NMR (75 MHz, CDCl$_3$): δ = 82.7 (*C*$_q$-OH), 41.6 (*CH$_2$*), 39.8 (2 × *CH$_2$*), 32.6 (*CH$_2$*), 24.5 (*CH$_2$*), 24.0 (2 × *CH$_2$*), 22.9 (*CH$_2$*), 14.2 (*CH$_3$*). – FTIR: ṽ = 3384, 2954, 2872, 1697, 1632, 1455, 1001 cm^{-1}. – MS (EI), m/z (%): 156 (4) [M$^+$], 127 (31) [(C$_8$H$_{15}$O)$^+$], 113 (29) [(C$_7$H$_{13}$O)$^+$], 99 (23) [(C$_6$H$_{11}$O)$^+$], 85 (100) [(C$_5$H$_9$O)$^+$], 67 (32), 58 (34). – HRMS (C$_{10}$H$_{20}$O): ber. 156.1514, gef. 156.1531.

2-Methyloct-3-yn-2-ol (**6e**): To a solution of 1-hexyne (4.11 g, 50.0 mmol, 1.00 eq.) in tetrahydrofurane (50 mL) was added 1.6 M butyllithium in hexane (34.4 mL, 3.52 g, 55.0 mmol, 1.10 eq.) at −78 °C. The reaction mixture was stirred for 1 hour at this temperature, then the solution was left to warm to room temperature. After that period the reaction mixture was cooled down to −78 °C again and then acetone (3.49 g, 60.0 mmol, 1.20 eq.) was added. The reaction mixture was left to warm up to room temperature and stirred overnight. The reaction mixture was quenched with water (20 mL) and washed three times with water. The organic layer was collected and dried over anhydrous $MgSO_4$. After filtration, the organic solvent was removed by evaporation under reduced pressure. The crude product was further purified by column chromatography using petroleum ether/ethyl acetat 10:1 as the eluent to give a colorless liquid (5.47 g, 78%). – ^{1}H-NMR (300 MHz, CDCl$_3$): δ = 2.17 (t, ^3J = 6.9 Hz, 2 H, C*H$_2$*), 1.96 (bs, 1 H, O*H*), 1.32–1.52 (m, 4 H, 2 × C*H$_2$*), 1.48 (s, 6 H, 2 × C*H$_3$*), 0.89 (t, ^3J = 7.0 Hz, 3 H, C*H$_3$*). – ^{13}C-NMR (75 MHz, CDCl$_3$): δ = 85.2 (*C*$_q$-*C*), 82.7 (*C*-CH$_2$), 65.4 (*C*$_q$-OH), 31.9 (2 × *CH$_3$*), 30.9 (*CH$_2$*), 22.0 (*CH$_2$*), 18.03 (*CH$_2$*), 13.7 (*CH$_3$*). – FTIR: ṽ = 3354, 2978, 2934, 2871, 2235, 1462, 1362, 1238, 1163, 944, 554 cm^{-1}. – MS (EI), m/z (%): 140 (1) [M$^+$], 125 (100) [(C$_8$H$_{13}$O)$^+$], 43 (100) [(C$_3$H$_7$)$^+$]. – HRMS (C$_9$H$_{16}$O): ber. 140.1201, gef. 140.1197.

1-(Hex-1-yn-1-yl)cyclohexanol (6f): To a solution of 1-hexyne (4.11 g, 50.0 mmol, 1.00 eq.) in tetrahydrofurane (100 mL) was added 1.6 M butyllithium in hexane (34.4 mL, 3.52 g, 55.0 mmol, 1.10 eq.) at −78 °C. The reaction mixture was stirred for 1 hour at this temperature, then the solution was left to warm to room temperature. After that period the reaction mixture was cooled down to −78 °C again and then cyclohexanone (5.89 g, 60.0 mmol, 1.20 eq.) was added. The reaction mixture was left to warm up to room temperature and stirred overnight. The reaction mixture was quenched with water (20 mL) and washed three times with water. The organic layer was collected and dried over anhydrous MgSO4. After filtration, the organic solvent was removed by evaporation under reduced pressure. The crude product was further purified by column chromatography using petroleum ether/ethyl acetat 10:1 as the eluent to give a yellow liquid (8.21 g, 91%). – ^{1}H-NMR (300 MHz, CDCl$_3$): δ = 2.21 (t, ^3J = 6.9 Hz, 2 H, CH_2), 1.80–1.91 (m, 2 H, CH_2), 1.77 (s, 1 H, OH), 1.60–1.72 (m, 2 H, CH_2), 1.23–1.58 (m, 10 H, 5 × CH_2), 0.90 (t, ^3J = 7.2 Hz, 3 H, CH_3).– ^{13}C-NMR (75 MHz, CDCl$_3$): δ = 84.8 (C$_q$-C), 84.0 (C-CH$_2$), 68.9 (C$_q$-OH), 40.4 (2 × CH$_2$), 31.0 (CH$_2$), 25.4 (CH$_2$), 23.6 (2 × CH$_2$), 22.0 (CH$_2$), 18.5 (CH$_2$), 13.7 (CH$_3$). – FTIR: ṽ = 3362, 2929, 2859, 1447, 1061, 963 cm^{-1}. – MS (EI), m/z (%): 180 (18) [M$^+$], 137 (100) [(C$_9$H$_{13}$O)$^+$]. – HRMS (C$_{11}$H$_{18}$O): ber. 180.1514, gef. 180.1521.

1-(Hex-1-yn-1-yl)cyclopentanol (6g): To a solution of 1-hexyne (4.11 g, 50.0 mmol, 1.00 eq.) in tetrahydrofurane (100 mL) was added 1.6 M butyllithium in hexane (34.4 mL, 3.52 g, 55.0 mmol, 1.10 eq.) at −78 °C. The reaction mixture was stirred for 1 hour at this temperature, then the solution was left to warm to room temperature. After that period the reaction mixture was cooled down to −78 °C again and then cyclopentanone (5.05 g, 60.0 mmol, 1.20 eq.) was added. The reaction mixture was left to warm up to room temperature and stirred overnight. The reaction mixture was quenched with water (20 mL) and washed three times with water. The organic layer was collected and dried over anhydrous MgSO$_4$. After filtration, the organic solvent was removed by evaporation under reduced pressure. The crude product was further purified by column chromatography using petroleum ether/ethyl acetat 10:1 as the eluent to give a yellow liquid (6.47 g, 78%). – ^{1}H-NMR (300 MHz, CDCl$_3$): δ = 2.19 (t, ^3J = 6.9 Hz, 2 H, CH_2), 1.64–1.89 (m, 9 H, OH + 4 × CH_2), 1.33–1.52 (m, 4 H, 2 × CH_2), 0.90 (t, ^3J = 7.1 Hz, 3 H, CH_3). – ^{13}C-NMR (75 MHz, CDCl$_3$): δ = 84.1 (C$_q$-C), 83.7 (C-CH$_2$), 74.9 (C$_q$-OH), 42.8 (2 × CH_2), 31.1 (CH_2), 23.5 (2 × CH_2), 22.1 (CH_2), 18.5 (CH_2), 13.8 (CH_3). – FTIR: ṽ = 3360, 2957, 2931, 2873, 2240, 1738, 1634, 993 cm^{-1}. – MS (EI), m/z (%): 166 (3) [M$^+$], 137
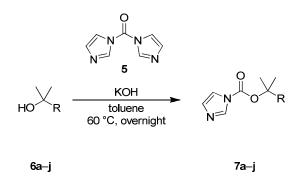
(100) [$(C_9H_{13}O)^+$], 124 (22) [$(C_8H_{12}O)^+$], 109 (26) [$(C_7H_9O)^+$]. – HRMS ($C_{11}H_{18}O$): ber. 166.1358, gef. 166.1368.

(*E*)-**Methylhex-3-en-2-ol** (**6h**): Methylmagnesium bromide (79.3 g, 300 mmol, 2.20 eq.) in diethyl ether (100 mL) was added slowly to a solution, cooled to 0 °C, of (*E*)-methyl pent-2-enoate (15.4 g, 135 mmol, 1.00 eq.) in diethyl ether (200 mL). The reaction mixture was stirred at room temperature overnight. The mixture was cooled to 0 °C again, quenched with ammonium sulfate solution (200 mL), washed with water and brine and dried over $MgSO_4$, filtered and concentrated. The crude product was further purified by column chromatography using petroleum ether/ethyl acetat 10:1 as the eluent to give a colorless oil (9.72 g, 63%). – ^{1}H-NMR (300 MHz, $CDCl_3$): δ = 5.66 (dt, ^3J = 15.7 Hz, ^3J = 5.4 Hz, 1 H, C*H*-CH$_2$), 5.58 (d, ^3J = 15.7 Hz, 1 H, C$_q$-C*H*), 2.03 (dq, ^3J = 7.4 Hz, ^3J = 5.4 Hz, 2 H, C*H*$_2$), 1.43 (bs, 1 H, O*H*), 1.30 (s, 6 H, 2 × C*H*$_3$), 0.98 (d, ^3J = 7.4 Hz, 3 H, C*H*$_3$). – ^{13}C-NMR (75 MHz, $CDCl_3$): δ = 137.0 (C$_q$-*C*H), 129.0 (*C*H-CH$_2$), 70.7 (HO-*C*$_q$), 30.0 (2 × *C*H$_3$), 25.3 (*C*H$_2$), 13.8 (*C*H$_3$). – FTIR: $\tilde{v}$ = 3354, 2966, 2932, 2874, 1461, 1372, 1361, 1234, 1147, 968, 908, 797cm^{-1}. – MS (EI), *m/z* (%): 114 (7) [M$^+$], 99 (51) [$(C_6H_{11}O)^+$], 85 (33), 59 (24), 43 (100) [$(C_3H_7)^+$]. – HRMS ($C_7H_{14}O$): ber. 114.1045, gef. 114.1061.

(*E*)-**2-Methyloct-3-en-2-ol** (**6i**): Methylmagnesium bromide (79.3 g, 300 mmol, 1.10 eq.) in diethyl ether (100 mL) was added slowly to a solution, cooled to 0 °C, of (*E*)-oct-3-en-2-one (34.3 g, 272 mmol, 1.00 eq.) in diethyl ether (250 mL). The reaction mixture was stirred at room temperature overnight. The mixture was cooled to 0 °C again, quenched with ammonium sulfate solution (200 mL), washed with water and brine and dried over $MgSO_4$, filtered and concentrated. The crude product was further purified by column chromatography using petroleum ether/ethyl acetat 5:1 as the eluent to give a yellow oil (29.1 g, 94%). – ^{1}H-NMR (300 MHz, $CDCl_3$): δ = 5.55–5.67 (m, 2 H, C*H*-CH$_2$ + C$_q$-C*H*), 1.98–2.04 (m, 2 H, C*H*$_2$), 1.37 (bs, 1 H, O*H*), 1.25–1.35 (m, 4 H, 2 × C*H*$_2$), 1.30 (s, 6 H, 2 × C*H*$_3$), 0.89 (t, ^3J = 7.0 Hz, 3 H, C*H*$_3$). – ^{13}C-NMR (75 MHz, $CDCl_3$): δ = 138.1 (C$_q$-*C*H), 127.5 (*C*H-CH$_2$), 70.8 (HO-*C*$_q$), 32.0 (*C*H$_2$), 31.6 (*C*H$_2$), 30.0 (2 × *C*H$_3$), 22.4 (*C*H$_2$), 14.1 (*C*H$_3$). – FTIR: $\tilde{v}$ = 3358, 2960, 2923, 2859, 1464, 1376, 1148, 969, 902 cm^{-1}. – MS (EI), *m/z* (%): 142 (9) [M$^+$], 127 (51) [$(C_8H_{15}O)^+$], 85 (59), 71 (100) [$(C_5H_{11})^+$]. – HRMS ($C_9H_{18}O$): ber. 142.1358, gef. 142.1362.

2-(3,5-Dimethylphenyl)propan-2-ol (**6j**): 3.0 M Methylmagnesium bromide (18.2 g, 68.8 mmol, 2.20 eq.) in diethyl ether (23 mL) was added slowly to a solution, cooled to 0 °C, of
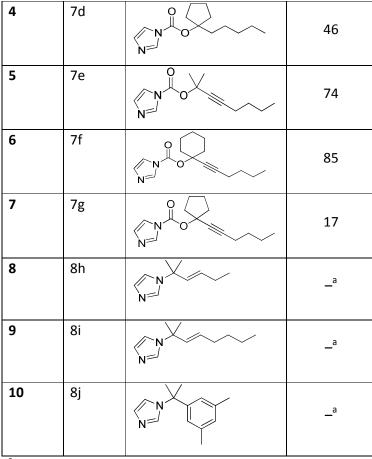
methyl 3,5-dimethylbenzoate (5.09 g, 31.0 mmol, 1.00 eq.) in diethyl ether (150 mL). The reaction mixture was stirred at room temperature overnight. The mixture was cooled to 0 °C again, quenched with ammonium sulfate solution (200 mL), washed with water and brine and dried over MgSO$_4$, filtered and concentrated. The crude product was further purified by column chromatography using petroleum ether/ethyl acetat 10:1 as the eluent to give a colorless oil (5.10 g, quant.). – ^{1}H-NMR (300 MHz, CDCl$_3$): δ = 7.12 (s, 2 H, 2 × C$_{ar}$H), 0.94 (s, 1 H, C$_{ar}$H), 2.35 (s, 6 H, 2 × C$_{ar}$-CH$_3$), 1.84 (s, 1 H, OH), 1.58 (s, 6 H, 2 × C$_q$-CH$_3$). – ^{13}C-NMR (75 MHz, CDCl$_3$): δ = 149.3 (C$_{ar}$-C$_q$), 137.9 (2 × C$_{ar}$-CH$_3$), 128.5 (C$_{ar}$H), 122.3 (2 × C$_{ar}$H), 72.6 (C$_q$-OH), 31.9 (2 × C$_q$-CH$_3$), 21.6 (2 × C$_{ar}$-CH$_3$). – FTIR: ṽ = 3388, 2975, 2918, 2867, 1727, 1603, 1451, 1363, 1159, 938, 848, 809, 706 cm^{-1}. – MS (EI), *m/z* (%): 164 (48) [M$^+$], 149 (100) [(C$_{10}$H$_{13}$O)$^+$]. – HRMS (C$_{11}$H$_{16}$O): ber. 164.1201, gef. 164.1185.
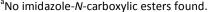

Scheme S2: Synthesis of imidazole-*N*-carboxylic esters **7a-j**.

Table S2: Overview of the imidazole-*N*-carboxylic **7a-j** esters prepared in this study.

Entry		Product	Yield [%]
1	7a		86
2	7b		70
3	7c		31

4	7d		46
5	7e		74
6	7f		85
7	7g		17
8	8h		—[a]
9	8i		—[a]
10	8j		—[a]

[a]No imidazole-*N*-carboxylic esters found.

*General procedure **A** for synthesis of imidazole-N-carboxylic esters **7***: To a solution of 1,1-carbonyldiimidazole (**5**) (1.10 eq.) in toluene (5.0 mL/mmol), alcohol **6a–j** (1.00 eq.) and potassium hydroxide (0.01 eq.) was added. The reaction mixture was stirred at 60 °C overnight. The solution was left to cool and concentrated in vacuo. The residue was dissolved in dichloromethane and washed three times with water. The organic layer was collected and dried over anhydrous MgSO$_4$. After filtration, the organic solvent was removed by evaporation under reduced pressure. The crude product was further purified by column chromatography using mixtures of petroleum ether/ethyl acetat as the eluent to give the imidazole-*N*-carboxylic esters **7a–g**.

2-Methylhexan-2-yl 1*H*-imidazole-1-carboxylate (**7a**): The reaction was carried out with 1,1-carbonyldiimidazole (**5**) (19.6 g, 110 mmol, 1.10 eq.), 2-methylhexan-2-ol (**6a**) (11.6 g, 100 mmol, 1.00 eq.) and potassium hydroxide (55.0 mg, 1.00 mmol, 0.01 eq.) according to general procedure **A**. The crude product was further purified by column chromatography

using petroleum ether/ethyl acetat 5:1 as the eluent to give a colorless liquid (18.0 g, 86%). –
^{1}H-NMR (300 MHz, CDCl$_3$): δ = 8.04 (s, 1 H, H_{ar}), 7.34 (s, 1 H, H_{ar}), 7.01 (s, 1 H, H_{ar}), 1.83–1.89
(m, 2 H, CH_2), 1.58 (s, 6 H, 2 × CH_3), 1.30–1.38 (m, 4 H, 2 × CH_2), 0.89–0.92 (m, 3 H, CH_3). –
^{13}C-NMR (75 MHz, CDCl$_3$): δ = 147.1 (C=O), 137.2 (C_{ar}H), 130.4 (C_{ar}H), 117.2 (C_{ar}H), 88.1 (O-
C_q), 40.6 (CH$_2$), 26.2 (CH$_2$), 25.9 (2 × CH$_3$), 22.6 (CH$_2$), 14.0 (CH$_3$). – FTIR: ṽ = 2958, 2934, 2871,
1754, 1470, 1379, 1319, 1285, 1241, 1218, 1182, 1149, 1092, 1057, 855, 836, 772, 763, 650,
599 cm^{-1}. – MS (EI), m/z (%): 210 (10) [M$^+$], 153 (18) [(C$_7$H$_9$N$_2$O$_2$)$^+$], 99 (100) [(C$_7$H$_{15}$)$^+$], 95 (45)
[(C$_4$H$_3$N$_2$O)$^+$]. – HRMS (C$_{11}$H$_{18}$N$_2$O$_2$): ber. 210.1368, gef. 210.1355.

1-Methylcyclohexyl 1H-imidazole-1-carboxylate (**7b**): The reaction was carried out with 1,1-
carbonyldiimidazole (**5**) (11.8 g, 66.0 mmol, 1.10 eq.), 1-methylcyclohexanol (**6b**) (6.85 g,
60.0 mmol, 1.00 eq.) and potassium hydroxide (34.0 mg, 600 µmol, 0.01 eq.) according to
general procedure **A**. The crude product was further purified by column chromatography
using petroleum ether/ethyl acetat 3:1 as the eluent to give a colorless solid (7.83 g, 63%). –
^{1}H-NMR (300 MHz, CDCl$_3$): δ = 8.07 (s, 1 H, H_{ar}), 7.36 (s, 1 H, H_{ar}), 7.01 (s, 1 H, H_{ar}), 2.20–2.30
(m, 2 H, CH_2), 1.25–1.63 (m, 8 H, 4 × CH_2), 1.60 (s, 3 H, CH_3). – ^{13}C-NMR (75 MHz, CDCl$_3$): δ =
147.0 (C=O), 137.1 (C_{ar}H), 130.4 (C_{ar}H), 117.1 (C_{ar}H), 87.3 (O-C_q), 36.5 (2 × CH$_2$), 25.4 (CH$_2$),
25.1 (CH$_3$), 22.2 (2 × CH$_2$). – FTIR: ṽ = 2933, 2862, 1748, 1469, 1447, 1378, 1318, 1298, 1275,
1231, 1182, 1146, 1092, 1058, 1000, 960, 867, 832, 770, 744, 651, 484 cm^{-1}. – MS (EI), m/z
(%): 208 (2) [M$^+$], 97 (52) [(C$_7$H$_{13}$)$^+$], 81 (100). – HRMS (C$_{11}$H$_{16}$N$_2$O$_2$): ber. 208.1212, gef.
208.1238.

1-Butylcyclopentyl 1H-imidazole-1-carboxylate (**7c**): The reaction was carried out with 1,1-
carbonyldiimidazole (5) (7.09 g, 35.0 mmol, 1.10 eq.), 1-butylcyclopentanol (6c) (3.98 g, 28.0
mmol, 1.00 eq.) and potassium hydroxide (16.0 mg, 280 µmol, 0.01 eq.) according to general
procedure A. The crude product was further purified by column chromatography using
petroleum ether/ethyl acetat 5:1 as the eluent to give a colorless solid (2.08 g, 31%). – [1]H-
NMR (300 MHz, CDCl$_3$): δ = 8.07 (s, 1 H, C$_{ar}H$), 7.37 (s, 1 H, C$_{ar}H$), 7.04 (s, 1 H, C$_{ar}H$), 2.23–2.34
(m, 2 H, CH_2), 2.04–2.10 (m, 2 H, CH_2), 1.66–1.84 (m, 6 H, 3 × CH_2), 1.27–1.37 (m, 4 H, 2 ×
CH_2), 0.89 (t, ^3J = 7.1 Hz, 3 H, CH_3). – ^{13}C-NMR (75 MHz, CDCl$_3$): δ = 145.4 (C=O), 137.2 (C_{ar}H),
130.5 (C_{ar}H), 117.2 (C_{ar}H), 98.8 (O-C_q), 37.6 (2 × CH$_2$), 36.8 (CH$_2$), 26.8 (CH$_2$), 24.0 (2 × CH$_2$),
23.0 (CH$_2$), 14.1 (CH$_3$). – FTIR: ṽ = 2959, 2872, 1752, 1469, 1382, 1286, 1239, 1171, 999, 772

cm^{-1}. – MS (ESI), *m/z* (%): 275 [(M+K)$^+$], 259 [(M+Na)$^+$], 236 [M$^+$]. – HRMS (C$_{13}$H$_{20}$N$_2$O$_2$Na): ber. 259.1422, gef. 259.1419. – HRMS (C$_{13}$H$_{20}$N$_2$O$_2$K): ber. 275.1162, gef. 275.1159.
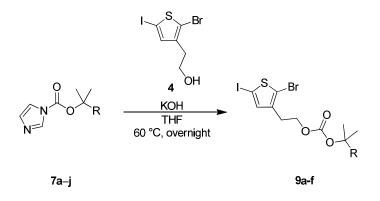
1-Pentylcyclopentyl 1*H*-imidazole-1-carboxylate (**7d**): The reaction was carried out with 1,1-carbonyldiimidazole (**5**) (1.96 g, 11.0 mmol, 1.10 eq.), 1-pentylcyclopentanol (**6d**) (1.56 g, 10.0 mmol, 1.00 eq.) and potassium hydroxide (6.00 mg, 100 μmol, 0.01 eq.) according to general procedure **A**. The crude product was further purified by column chromatography using petroleum ether/ethyl acetat 5:1 as the eluent to give a colorless solid (1.16 g, 46%). – ^{1}H-NMR (300 MHz, CDCl$_3$): δ = 8.05 (s, 1 H, C$_{ar}$*H*), 7.36 (s, 1 H, C$_{ar}$*H*), 7.03 (s, 1 H, C$_{ar}$*H*), 2.20–2.33 (m, 2 H, C*H$_2$*), 2.02–2.08 (m, 2 H, C*H$_2$*), 1.65–1.82 (m, 6 H, 3 × C*H$_2$*), 1.22–1.38 (m, 6 H, 3 × C*H$_2$*), 0.85 (t, ^3J = 7.0 Hz, 3 H, C*H$_3$*). – ^{13}C-NMR (75 MHz, CDCl$_3$): δ = 147.5 (*C*=O), 137.2 (*C$_{ar}$*H), 130.5 (*C$_{ar}$*H), 117.3 (*C$_{ar}$*H), 98.9 (O-*C$_q$*), 37.5 (2 × *C*H$_2$), 37.0 (*C*H$_2$), 32.1 (*C*H$_2$), 24.3 (*C*H$_2$), 24.0 (2 × *C*H$_2$), 22.6 (*C*H$_2$), 14.6 (*C*H$_3$), – FTIR: ṽ = 2957, 2865, 1749, 1467, 1378, 1282, 1236, 1165, 1093, 1000, 771, 651 cm^{-1}. – MS (ESI), *m/z* (%): 523 (73) [(2M+Na)$^+$]. – HRMS (C$_{28}$H$_{44}$N$_4$NaO$_4$): ber. 523.3260, gef. 523.3267.

2-Methyloct-3-yn-2-yl 1*H*-imidazole-1-carboxylate (**7e**): The reaction was carried out with 1,1-carbonyldiimidazole (**5**) (1.41 g, 7.92 mmol, 1.10 eq.), 2-methyloct-3-yn-2-ol (**6e**) (1.01 g, 7.20 mmol, 1.00 eq.) and potassium hydroxide (4.00 mg, 72.0 μmol, 0.01 eq.) according to general procedure **A**. The crude product was further purified by column chromatography using petroleum ether/ethyl acetat 10:1 as the eluent to give a colorless solid (1.25 g, 74%). – ^{1}H-NMR (300 MHz, CDCl$_3$): δ = 8.08 (s, 1 H, *H$_{ar}$*), 7.38 (s, 1 H, *H$_{ar}$*), 7.03 (s, 1 H, *H$_{ar}$*), 2.21 (t, ^3J = 7.0 Hz, 2 H, C*H$_2$*), 1.79 (s, 6 H, 2 × C*H$_3$*), 1.32–1.53 (m, 4 H, 2 × C*H$_2$*), 0.89 (t, ^3J = 7.2 Hz, 3 H, C*H$_3$*). – ^{13}C-NMR (75 MHz, CDCl$_3$): δ = 146.7 (*C*=O), 137.3 (*C$_{ar}$*H), 130.5 (*C$_{ar}$*H), 117.3 (*C$_{ar}$*H), 87.3 (C$_q$-*C*), 79.8 (*C*-CH$_2$), 77.7 (O-*C$_q$*), 30.6 (*C*H$_2$), 29.5 (2 × *C*H$_3$), 22.0 (*C*H$_2$), 18.5 (*C*H$_2$), 13.7 (*C*H$_3$). – FTIR: ṽ = 2989, 2933, 2689, 2247, 1763, 1468, 1379, 1291, 1241, 1125, 1091, 998, 839, 769, 649 cm^{-1}. – MS (EI), *m/z* (%): 234 (4) [M$^+$], 123 (100) [(C$_9$H$_{15}$)$^+$], 81 (71) [(C$_6$H$_9$)$^+$]. – HRMS (C$_{13}$H$_{18}$N$_2$O$_2$): ber. 234.1368, gef. 234.1366.

1-(Hex-1-yn-1-yl)cyclohexyl 1*H*-imidazole-1-carboxylate (**7f**): The reaction was carried out with 1,1-carbonyldiimidazole (**5**) (4.41 g, 24.8 mmol, 1.10 eq.), 1-(hex-1-yn-1-yl)cyclohexanol (**6f**) (4.06 g, 22.5 mmol, 1.00 eq.) and potassium hydroxide (13.0 mg, 225 μmol, 0.01 eq.) according to general procedure **A**. The crude product was further purified by column chromatography using petroleum ether/ethyl acetat 5:1 as the eluent to give a colorless
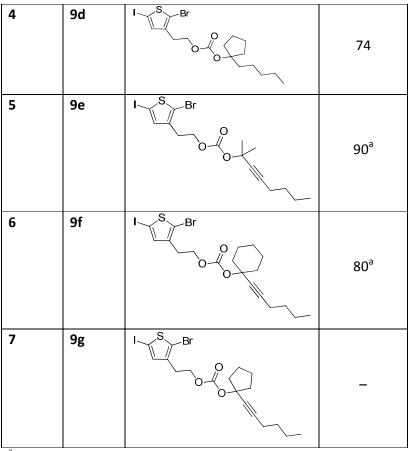
solid (5.24 g, 85%). – ^{1}H-NMR (300 MHz, CDCl$_3$): δ = 8.10 (s, 1 H, H_{ar}), 7.40 (s, 1 H, H_{ar}), 7.04

(s, 1 H, H_{ar}), 2.17–2.28 (m, 4 H, 2 × CH_2), 1.94–2.04 (m, 2 H, CH_2), 1.30–1.71 (m, 10 H, 5 ×

CH_2), 0.90 (t, ^3J = 7.2 Hz, 3 H, CH_3). – ^{13}C-NMR (75 MHz, CDCl$_3$): δ = 146.3 (*C*=O), 137.2 (C_{ar}H),

130.4 (C_{ar}H), 117.2 (C_{ar}H), 89.0 (C$_q$-*C*), 81.2 (*C*-C), 78.5 (C$_q$), 37.5 (2 × *C*H$_2$), 30.6 (*C*H$_2$), 25.0

(*C*H$_2$), 22.9 (2 × *C*H$_2$), 22.0 (*C*H$_2$), 18.5 (*C*H$_2$), 13.6 (*C*H$_3$). – FTIR: ṽ = 2934, 2860, 2240, 1763,

1467, 1378, 1283, 1234, 1167, 1092, 996, 893, 830, 765, 742, 649 cm^{-1}. – MS (ESI), *m/z* (%):

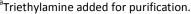313 [(M+K)$^+$], 297 [(M+Na)$^+$]. – HRMS (C$_{16}$H$_{22}$N$_2$O$_2$Na): ber. 297.1579, gef. 297.1574.

Scheme S3: Synthesis of carbonates **9a-g**.

Table S3: Thiophene monomers **9a-g** prepared in this study.

Entry		Product	Yield [%]
1	**9a**		86
2	**9b**		84
3	**9c**		91

4	9d		74
5	9e		90[a]
6	9f		80[a]
7	9g		–

[a]Triethylamine added for purification.

*General procedure **B** for synthesis of thiophene monomers **9***: To a solution of imidazole-*N*-carboxylic esters (**7a–f**) (1.10 eq.) and potassium hydroxide (0.01 eq.) in tetrahydrofuran (4.0 mL/mmol), 2-(2-bromo-5-iodothiophen-3-yl)ethanol (**4**) (1.00 eq.) in tetrahydrofuran (10 mL) was added dropwise. The reaction mixture was stirred at 60 °C overnight. The solution was left to cool and concentrated in vacuo. The residue was dissolved in dichloromethane and washed three times with water. The organic layer was collected and dried over anhydrous MgSO$_4$. After filtration, the organic solvent was removed by evaporation under reduced pressure. The crude product was further purified by column chromatography using mixtures of petroleum ether/ethyl acetat as the eluent to give the thiophene monomers **9a–g**.

2-(2-Bromo-5-iodothiophen-3-yl)ethyl (2-methylhexan-2-yl) carbonate (**9a**): The reaction was carried out with 2-methylhexan-2-yl 1*H*-imidazole-1-carboxylate (**7a**) (694 mg, 3.30 mmol, 1.10 eq.), 2-(2-bromo-5-iodothiophen-3-yl)ethanol (**4**) (1.00 g, 3.00 mmol, 1.00 eq.) and potassium hydroxide (2.00 mg, 30.0 µmol, 0.01 eq.) according to general procedure **B**.

The crude product was further purified by column chromatography using petroleum ether/ethyl acetat 10:1 as the eluent to give a colorless oil (1.23 g, 86%). – ^{1}H-NMR (300 MHz, CDCl$_3$): δ = 7.02 (s, 1 H, H_{ar}), 4.20 (t, ^3J = 6.9 Hz, 2 H, CH_2-O), 2.91 (t, ^3J = 6.9 Hz, 2 H, C$_{ar}$-CH_2), 1.73–1.78 (m, 2 H, C$_q$-CH_2), 1.45 (s, 6 H, 2 × CH_3), 1.26–1.35 (m, 4 H, 2 × CH_2), 0.91 (t, ^3J = 6.7 Hz, 3 H, CH_3). – ^{13}C-NMR (75 MHz, CDCl$_3$): δ = 153.4 (C=O), 139.3 (C_{ar}-CH$_2$), 138.2 (C_{ar}), 113.7 (C_{ar}-Br), 84.7 (O-C_q), 71.7 (C_{ar}-I), 65.3 (CH$_2$-O), 40.4 (C$_q$-CH$_2$), 28.9 (C_{ar}-CH$_2$), 26.2 (CH$_2$), 25.8 (2 × CH$_3$), 23.1 (CH$_2$), 14.2 (CH$_3$). – FTIR: ṽ = 2955, 2930, 2865, 1736, 1456, 1385, 1369, 1271, 1249, 1213, 1154, 1092, 1074, 984, 957, 869, 826, 791, 472 cm^{-1}. – MS (EI), m/z (%): 476/474 (9/9) [M$^+$], 316/314 (100/94) [(C$_6$H$_4$BrIS)$^+$]. – HRMS (C$_{14}$H$_{20}$BrIO$_3$S): ber. 473.9361, gef. 473.9370.

2-(2-Bromo-5-iodothiophen-3-yl)ethyl (1-cyclohexyl) carbonate (**9b**): The reaction was carried out with 1-methylcyclohexyl 1H-imidazole-1-carboxylate (**7b**) (687 mg, 3.30 mmol, 1.10 eq.), 2-(2-bromo-5-iodothiophen-3-yl)ethanol (**4**) (1.00 g, 3.00 mmol, 1.00 eq.) and potassium hydroxide (2.00 mg, 30.0 µmol, 0.01 eq.) according to general procedure **B**. The crude product was further purified by column chromatography using petroleum ether/ethyl acetat 5:1 as the eluent to give a yellow oil (1.19 g, 84%). – ^{1}H-NMR (300 MHz, CDCl$_3$): δ = 7.03 (s, 1 H, H_{ar}), 4.21 (t, ^3J = 7.0 Hz, 2 H, CH_2-O), 2.92 (t, ^3J = 7.0 Hz, 2 H, C$_{ar}$-CH_2), 2.08–2.15 (m, 2 H, C$_q$-CH_2), 1.20–1.61 (m, 8 H, 4 × CH_2), 1.48 (s, 3 H, CH_3). – ^{13}C-NMR (75 MHz, CDCl$_3$): δ = 153.3 (C=O), 139.4 (C_{ar}-CH$_2$), 138.3 (C_{ar}), 113.7 (C_{ar}-Br), 84.0 (O-C_q), 71.7 (C_{ar}-I), 65.3 (CH$_2$-O), 36.6 (2 × CH$_2$), 27.1 (CH$_2$), 25.5 (C_{ar}-CH$_2$), 25.2 (CH$_3$), 22.3 (2 × CH$_2$). – FTIR: ṽ = 2931, 2859, 1734, 1445, 1228 cm^{-1}. – MS (EI), m/z (%): 474/472 (6/5) [M$^+$], 316/314 (100/94) [(C$_6$H$_4$BrIS)$^+$]. – HRMS (C$_{14}$H$_{18}$BrIO$_3$S): ber. 471.9205, gef. 471.9199.
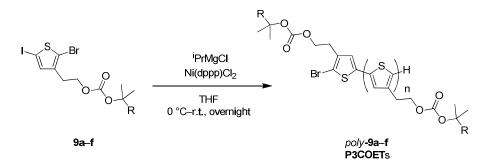
2-(2-Bromo-5-iodothiophen-3-yl)ethyl (1-butylcyclopentyl) carbonate (**9c**): The reaction was carried out with 1-butylcyclopentyl 1H-imidazole-1-carboxylate (**7c**) (1.01 g, 4.30 mmol, 1.10 eq.), 2-(2-bromo-5-iodothiophen-3-yl)ethanol (**4**) (1.30 g, 3.90 mmol, 1.00 eq.) and potassium hydroxide (2.00 mg, 39.0 µmol, 0.01 eq.) according to general procedure **B**. The crude product was further purified by column chromatography using petroleum ether/ethyl acetat 10:1 as the eluent to give a colorless oil (1.77 g, 91%). – ^{1}H-NMR (300 MHz, CDCl$_3$): δ = 7.02 (s, 1 H, H_{ar}), 4.21 (t, ^3J = 6.7 Hz, 2 H, CH_2-O), 2.91 (t, ^3J = 6.7 Hz, 2 H, C$_{ar}$-CH_2), 2.07–2.18 (m, 2 H, C$_q$-CH_2), 1.89–1.97 (m, 2 H, CH_2), 1.57–1.79 (m, 6 H, 3 × CH_2), 1.25–1.35 (m, 4 H, 2 × CH_2), 0.90 (t, ^3J = 6.9 Hz, 3 H, CH_3). – ^{13}C-NMR (75 MHz, CDCl$_3$): δ = 153.5 (C=O), 139.3 (C_{ar}-

CH$_2$), 138.2 (C$_{ar}$H), 113.7 (C$_{ar}$-Br), 95.5 (O-C$_q$), 71.8 (C$_{ar}$-I), 65.4 (CH$_2$-O), 37.5 (2 × CH$_2$), 36.7 (CH$_2$), 29.0 (CH$_2$), 27.1 (CH$_2$), 24.1 (2 × CH$_2$), 23.1 (CH$_2$), 14.2 (CH$_3$). − FTIR: ṽ = 2959, 2870, 1735, 1453, 1388, 1251, 1172, 1102, 965, 792 cm^{-1}. − MS (Fab), m/z (%): 502/500 [M$^+$]. − HRMS (C$_{16}$H$_{22}$BrIO$_3$S): ber. 499.9518, gef. 499.9489.

2-(2-Bromo-5-iodothiophen-3-yl)ethyl (1-pentylcyclopentyl) carbonate (**9d**): The reaction was carried out with 1-butylcyclopentyl 1H-imidazole-1-carboxylate (**7d**) (1.01 g, 4.30 mmol, 1.10 eq.), 2-(2-bromo-5-iodothiophen-3-yl)ethanol (**4**) (1.30 g, 3.90 mmol, 1.00 eq.) and potassium hydroxide (2.00 mg, 39.0 µmol, 0.01 eq.) according to general procedure **B**. The crude product was further purified by column chromatography using petroleum ether/ethyl acetat 10:1 as the eluent to give a colorless oil (1.77 g, 91%). − ^{1}H-NMR (300 MHz, CDCl$_3$): δ = 7.02 (s, 1 H, H_{ar}), 4.20 (t, ^3J = 7.0 Hz, 2 H, CH$_2$-O), 2.90 (t, ^3J = 7.0 Hz, 2 H, C$_{ar}$-CH$_2$), 2.06–2.17 (m, 2 H, C$_q$-CH$_2$), 1.89–1.95 (m, 2 H, CH$_2$), 1.57–1.77 (m, 6 H, 3 × CH$_2$), 1.23–1.36 (m, 6 H, 3 × CH$_2$), 0.87 (t, ^3J = 6.6 Hz, 3 H, CH$_3$). − ^{13}C-NMR (75 MHz, CDCl$_3$): δ = 153.5 (C=O), 139.3 (C$_{ar}$-CH$_2$), 138.2 (C$_{ar}$H), 113.6 (C$_{ar}$-Br), 95.5 (O-C$_q$), 71.7 (C$_{ar}$-I), 65.4 (CH$_2$-O), 37.5 (CH$_2$), 36.9 (2 × CH$_2$), 32.2 (CH$_2$), 28.9 (CH$_2$), 24.2 (CH$_2$), 24.1 (2 × CH$_2$), 22.7 (CH$_2$), 14.2 (CH$_3$). − FTIR: ṽ = 2954, 2865, 1735, 1454, 1259, 1201, 983, 792 cm^{-1}. − MS (ESI), m/z (%): 554/552 [(M+K)$^+$]. − HRMS (C$_{17}$H$_{24}$BrIO$_3$SK): ber. 552.9311, gef. 552.9312.

2-(2-Bromo-5-iodothiophen-3-yl)ethyl (2-methyloct-3-yn-2-yl) carbonate (**9e**): The reaction was carried out with 2-methyloct-3-yn-2-yl 1H-imidazole-1-carboxylate (**7e**) (1.29 g, 5.50 mmol, 1.10 eq.), 2-(2-bromo-5-iodothiophen-3-yl)ethanol (**4**) (1.67 g, 5.00 mmol, 1.00 eq.) and potassium hydroxide (3.00 mg, 50.0 µmol, 0.01 eq.) according to general procedure **B**. The crude product was further purified by column chromatography using petroleum ether/ethyl acetat 10:1 and triethylamine (2 vol.-%) as the eluent to give a yellow oil (2.25 g, 90%). − ^{1}H-NMR (300 MHz, CDCl$_3$): δ = 7.03 (s, 1 H, H_{ar}), 4.23 (t, ^3J = 6.9 Hz, 2 H, CH$_2$-O), 2.92 (t, ^3J = 6.9 Hz, 2 H, C$_{ar}$-CH$_2$), 2.21 (t, ^3J = 6.9 Hz, 2 H, C-CH$_2$), 1.67 (s, 6 H, 2 × CH$_3$), 1.33–1.53 (m, 4 H, 2 × CH$_2$), 0.90 (t, ^3J = 7.1 Hz, 3 H, CH$_3$). − ^{13}C-NMR (75 MHz, CDCl$_3$): δ = 152.9 (C=O), 139.3 (C$_{ar}$-CH$_2$), 138.2 (C$_{ar}$H), 113.7 (C$_{ar}$-Br), 85.6 (C-CH$_2$), 80.7 (C-C$_q$), 75.3 (O-C$_q$), 71.7 (C$_{ar}$-I), 65.7 (CH$_2$-O), 30.7 (CH$_2$), 29.3 (2 × CH$_3$), 28.9 (CH$_2$), 22.0 (CH$_2$), 18.5 (CH$_2$), 13.7 (CH$_3$). − FTIR: ṽ = 2958, 2930, 2867, 2245, 1748, 1463, 1384, 1250, 1194, 1132, 1100, 790 cm^{-1}. − MS (EI), m/z (%): 500/498 (12/12) [M$^+$], 316/314 (100/95) [(C$_6$H$_4$BrIS)$^+$], 236 (25) [(C$_6$H$_5$IS)$^+$], 123 (61) [(C$_9$H$_{15}$)$^+$]. − HRMS (C$_{16}$H$_{20}$BrIO$_3$S): ber. 497.9361, gef. 497.9385.

2-(2-Bromo-5-iodothiophen-3-yl)ethyl (1-(hex-1-yn-1-yl)cyclohexyl) carbonate (**9f**): The reaction was carried out with 1-(hex-1-yn-1-yl)cyclohexyl 1*H*-imidazole-1-carboxylate (**7f**) (1.51 g, 5.50 mmol, 1.10 eq.), 2-(2-bromo-5-iodothiophen-3-yl)ethanol (**4**) (1.67 g, 5.00 mmol, 1.00 eq.) and potassium hydroxide (3.00 mg, 50.0 μmol, 0.01 eq.) according to general procedure **B**. The crude product was further purified by column chromatography using petroleum ether/ethyl acetat 20:1 and triethylamine (2 vol.-%) as the eluent to give a yellow oil (2.17 g, 80%). – ^{1}H-NMR (300 MHz, CDCl$_3$): δ = 7.03 (s, 1 H, H_{ar}), 4.24 (t, ^3J = 7.2 Hz, 2 H, CH_2-O), 2.93 (t, ^3J = 7.2 Hz, 2 H, C$_{ar}$-CH_2), 2.25 (t, ^3J = 7.2 Hz, 2 H, C-CH_2), 2.09–2.17 (m, 2 H, CH_2), 1.77–1.86 (m, 2 H, CH_2), 1.60–1.68 (m, 4 H, 2 × CH_2), 1.39–1.45 (m, 6 H, 3 × CH_2), 0.91 (t, ^3J = 7.2 Hz, 3 H, CH_3). – ^{13}C-NMR (75 MHz, CDCl$_3$): δ = 152.8 (*C*=O), 139.3 (*C*$_{ar}$-CH$_2$), 138.2 (*C*$_{ar}$H), 113.7 (*C*$_{ar}$-Br), 87.9 (*C*-CH$_2$), 79.5 (*C*-C$_q$), 79.0 (O-*C*$_q$), 71.9 (*C*$_{ar}$-I), 65.7 (*C*H$_2$-O), 37.5 (2 × *C*H$_2$), 30.9 (*C*H$_2$), 27.1 (*C*H$_2$), 25.3 (2 × *C*H$_3$), 23.1 (*C*H$_2$), 22.1 (*C*H$_2$), 18.7 (*C*H$_2$), 13.8 (*C*H$_3$). – FTIR: ṽ = 2930, 2857, 2240, 1745, 1447, 1267, 1231, 1182, 1125, 1014, 917, 782 cm^{-1}. – MS (FAB), *m/z* (%): 541/539 (67/100) [(M+H)$^+$], 540/538 (50/47) [M$^+$]. – HRMS (C$_{19}$H$_{24}$BrIO$_3$S): ber. 537.9674, gef. 537.9725.

Scheme S4: KCT Polymerization of carbonates **9a-f**.

*General procedure **C** for synthesis of* **P3COET**s *poly-9*: A solution of thiophene monomers (**9a–f**) (1.00 eq.) in tetrahydrofuran (5.0 mL/mmol) was stirred at 0 °C. To the mixture was added a 2.0 M isopropylmagnesium chloride solution in diethyl ether (1.00 eq.) and the mixture was stirred at 0 °C for 1 h. Then a suspension of 1,3-bis(diphenylphosphino)propane nickel(II) chloride (0.005 eq.) in tetrahydrofuran (5.0 mL) was added to the mixture at 0 °C, and then the mixture was stirred at room temperature. After the reaction mixture had been

stirred for 24 h, 5 M hydrochloric acid was added and the mixture was extracted with chloroform. The organic layer was washed with water, dried over anhydrous $MgSO_4$, and concentrated under reduced pressure. The product was redissolved in chloroform and was poured in methanol. The insoluble material was purified by Soxhlet extraction (methanol, acetone, chloroform) to give the polythiophenes *poly*-**9a–f**.

Poly(2-methylhexan-2-yl 2-(thiophen-3-yl)ethyl carbonate) (*poly*-**9a**): The reaction was carried out with 2-(2-bromo-5-iodothiophen-3-yl)ethyl (2-methylhexan-2-yl) carbonate (**9a**) (4.66 g, 9.80 mmol, 1.00 eq.), 2.0 M isopropylmagnesium chloride solution (4.9 mL, 1.01 g, 9.80 mmol, 1.00 eq.) and 1,3-bis(diphenylphosphino)propane nickel(II) chloride (27.0 mg, 49.0 µmol, 0.005 eq.) according to general procedure **C**. The crude product was further purified by Soxhlet extraction to give a red solid (acetone: 1.02 g, 39%; chloroform: 382 mg, 15%). − ^{1}H-NMR (300 MHz, $CDCl_3$): δ = 7.10 (s, 1 H, H_{ar}), 4.36 (m, 2 H, CH_2-O), 3.18 (m, 2 H, C_{ar}-CH_2), 1.73–1.81 (m, 2 H, C_q-CH_2), 1.46 (s, 6 H, 2 × CH_3), 1.26–1.35 (m, 4 H, 2 × CH_2), 0.85–0.92 (m, 3 H, CH_3). − SEC (PSS-standard): acetone: M_n = 15.3 kg mol^{-1}, M_w = 24.6 kg mol^{-1}, PDI = 1.61; Chloroform: M_n = 41.0 kg mol^{-1}, M_w = 45.6 kg mol^{-1}, PDI = 1.11. − FTIR: $\tilde{v}$ = 2955, 2932, 2865, 1733, 1456, 1386, 1368, 1269, 1246, 1212, 1153, 1073, 938, 862, 831, 790 cm^{-1}. − TGA/DSC (10 K/min, 5% weight loss): 192°C. − UV-Vis (chloroform): absorption: solution = 437 nm, film = 475 nm; emission: solution = 563 nm, film = 628 nm. − CV (as film against Fc/Fc$^+$ in acetonitrile): E^{ox} = 0.518 V.

Poly(1-methylcyclohexyl 2-(thiophen-3-yl)ethyl carbonate) (*poly*-**9b**): The reaction was carried out with 2-(2-bromo-5-iodothiophen-3-yl)ethyl (1-methylcyclohexyl) carbonate (**9b**) (1.11 g, 2.35 mmol, 1.00 eq.), 2.0 M isopropylmagnesium chloride solution (1.1 mL, 242 mg, 2.35 mmol, 1.00 eq.) and 1,3-bis(diphenylphosphino)propane nickel(II) chloride (6.00 mg, 12.0 µmol, 0.005 eq.) according to general procedure **C**. The crude product was further purified by Soxhlet extraction to give a red solid (chloroform: 165 mg, 26%). − ^{1}H-NMR (300 MHz, $CDCl_3$): δ = 7.11 (s, 1 H, H_{ar}), 4.30–4.40 (m, 2 H, CH_2-O), 3.12–3.21 (m, 2 H, C_{ar}-CH_2), 2.08–2.17 (m, 2 H, C_q-CH_2), 1.41–1.59 (m, 11 H, 4 × CH_2 + CH_3). − SEC (PSS-standard): acetone: M_n = 5.51 kg mol^{-1}, M_w = 7.28 kg mol^{-1}, PDI = 1.32; Chloroform: M_n = 18.4 kg mol^{-1}, M_w = 22.9 kg mol^{-1}, PDI = 1.25. − FTIR: $\tilde{v}$ = 2930, 2859, 1732, 1444, 1372, 1294, 1263, 1228, 1150, 1088, 1040, 957, 870, 793 cm^{-1}. − TGA/DSC (10 K/min, 5% weight loss): 194 °C. − UV-Vis (chloroform): absorption: solution = 436 nm; emission: solution = 562 nm.

Poly(1-butylcyclopentyl 2-(thiophen-3-yl)ethyl carbonate) (*poly*-**9c**): The reaction was carried out with 2-(2-bromo-5-iodothiophen-3-yl)ethyl (1-butylcyclopentyl) carbonate (**9c**) (1.55 g, 3.10 mmol, 1.00 eq.), 2.0 M isopropylmagnesium chloride solution (1.6 mL, 319 mg, 3.10 mmol, 1.00 eq.) and 1,3-bis(diphenylphosphino)propane nickel(II) chloride (8.00 mg, 16.0 µmol, 0.005 eq.) according to general procedure **C**. The crude product was further purified by Soxhlet extraction to give a red solid (chloroform: 85.0 mg, 5%). − SEC (PSS-standard): chloroform: M_n = 22.2 kg mol^{-1}, M_w = 27.5 kg mol^{-1}, PDI = 1.24. − FTIR: $\tilde{v}$ = 2954, 2866, 134, 1452, 1251, 960 cm^{-1}. − TGA/DSC (10 K/min, 5% weight loss): 140 °C. − UV-Vis (chloroform): absorption: solution = 430 nm; emission: solution = 562 nm.

Poly(1-pentylcyclopentyl 2-(thiophen-3-yl)ethyl carbonate) (*poly*-**9d**): The reaction was carried out with 2-(2-bromo-5-iodothiophen-3-yl)ethyl (1-pentylcyclopentyl) carbonate (**9d**) (2.72 g, 5.30 mmol, 1.00 eq.), 2.0 M isopropylmagnesium chloride solution (2.7 mL, 545 mg, 5.30 mmol, 1.00 eq.) and 1,3-bis(diphenylphosphino)propane nickel(II) chloride (14.0 mg, 27.0 µmol, 0.005 eq.) according to general procedure **C**. The crude product was further purified by Soxhlet extraction to give a red solid (acetone: 30.0 mg, 3%). − SEC (PSS-standard): acetone: M_n = 4.33 kg mol^{-1}, M_w = 4.83 kg mol^{-1}, PDI = 1.12. − FTIR: $\tilde{v}$ = 2955, 2926, 2856, 1737, 1456, 1257, 1009, 791 cm^{-1}. − TGA/DSC (10 K/min, 5% weight loss): 168 °C. − UV-Vis (chloroform): absorption: solution = 429 nm; emission: solution = 562 nm.

Poly(2-methyloct-3-yn-2-yl 2-(thiophen-3-yl)ethyl carbonate) (*poly*-**9e**): The reaction was carried out with 2-(2-bromo-5-iodothiophen-3-yl)ethyl (2-methyloct-3-yn-2-yl) carbonate (**9e**) (2.50 g, 5.00 mmol, 1.00 eq.), 2.0 M isopropylmagnesium chloride solution (2.5 mL, 514 mg, 5.00 mmol, 1.00 eq.) and 1,3-bis(diphenylphosphino)propane nickel(II) chloride (14.0 mg, 25.0 µmol, 0.005 eq.) according to general procedure **C**. The crude product was further purified by Soxhlet extraction to give a red solid (chloroform: 290 mg, 20%). − SEC (PSS-standard): acetone: M_n = 8.23 kg mol^{-1}, M_w = 10.9 kg mol^{-1}, PDI = 1.32. − FTIR: $\tilde{v}$ = 2959, 2867, 1745, 1461, 1383, 1250, 1129, 1096, 783 cm^{-1}. − TGA/DSC (10 K/min, 5% weight loss): 174 °C. UV-Vis (chloroform): absorption: solution = 431 nm, film = 474 nm; emission: solution = 561 nm, film = 609 nm.

Poly(1-(hex-1-yn-1-yl)cyclohexyl 2-(thiophen-3-yl)ethyl carbonate) (*poly*-**9f**): The reaction was carried out with 2-(2-bromo-5-iodothiophen-3-yl)ethyl (1-(hex-1-yn-1-yl)cyclohexyl) carbonate (**9f**) (1.89 g, 3.50 mmol, 1.00 eq.), 2.0 M isopropylmagnesium chloride solution

(1.8 mL, 360 mg, 3.50 mmol, 1.00 eq.) and 1,3-bis(diphenylphosphino)propane nickel(II) chloride (9.00 mg, 18.0 µmol, 0.005 eq.) according to general procedure **C**. The crude product was further purified by Soxhlet extraction to give a red solid (acetone: 273 mg, 23%). – SEC (PSS-standard): acetone: M_n = 17.9 kg mol^{-1}, M_w = 31.7 kg mol^{-1}, PDI = 1.77. – FTIR: $\tilde{v}$ = 2929, 2856, 1744, 1447, 1264, 127, 1179, 1009, 894, 790 cm^{-1}. – TGA/DSC (10 K/min, 5% weight loss): 178 °C. – UV-Vis (chloroform): absorption: solution = 428 nm; emission: solution = 560 nm.
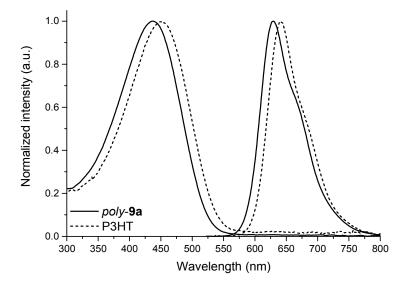

Figure S1: Normalized absorption and emission spectra of P3COETs poly-9a (solid) and P3HT (dashed).

S2. Grazing Incidence Wide Angle X-ray Scattering (GIWAXS)

GIWAXS measurements of *poly*-**9a** drop cast films were performed at the DELTA Synchrotron using beamline BL09 with a photon energy of 10 keV (λ = 1.2398 Å^{-1}). The scattering intensity was detected on a 2-D image plate (MAR-345) with a pixel size of 150 µm (2300 × 2300 pixels), and the detector was placed 345mm from the sample center. Data analysis was performed using the Datasqueeze software. The beam size was 0.05 mm × 0.5 mm and samples were irradiated just below the critical angle for total reflection with respect to the incoming X-ray beam (~ 0.18 °).

GIWAXS experiments of the sample in OPV architecture and for *poly*-**9a** spin coated film were performed by means of a solid anode X-ray tube (Siemens Kristalloflex X-ray source, copper anode X-ray tube operated at 30 kV and 20 mA). Osmic confocal MaxFlux optics, X-ray beam with pinhole collimation and a MAR345 image plate detector. The samples were prepared as thin film with the same procedure as it was used in OPVs fabrication with one change as a substrate the silicon/silicon dioxide was used.
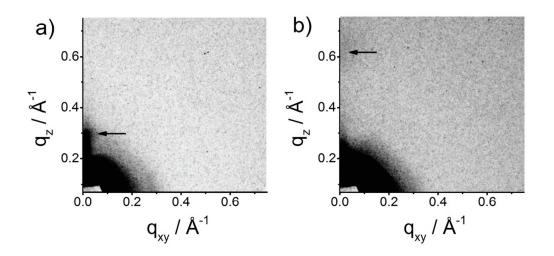

Figure S2. GIWAXS patterns of thin films of spin coated **P3COET** *poly*-**9a** after annealing (a) at 100 °C and (b) after annealing at 150 °C (72 h). Meridional reflection related to the interlayer structure is indicated by black arrows in the GIWAXS patterns.

S3. Field-Effect Transistors

To find the relation between thermal cleavage and charge carrier mobility, *poly*-**9a** has been employed as an exemplary active material in transistors. The field-effect transistors (FET) were processed using bottom gate, bottom contact architecture with gold source and drain electrodes. The 300 nm thick SiO_2 dielectric covering the highly doped Si acting as the gate electrode was functionalized with hexamethyldisilazane (HMDS) to minimize interfacial trapping sites. *Poly*-**9a** thin films were deposited by drop-casting 2 mg/mL chloroform solution on FET substrates in nitrogen atmosphere. The channel lengths and widths are 10 and 700 mm, respectively. All the fabrication procedures and electrical measurements (using Keithley 4200 SCS) were performed in a glove box under nitrogen atmosphere.

In order to compare the charge carrier transport before and after thermal cleavage, FETs were measured after thermal annealing at two different temperatures: below (100 °C), to ensure evaporation of residual solvent and order improvement by polymer reorganization,

and at 200°C, *i.e.,* above the cleavage temperature (192 °C). Transfer characteristics presented on Figure S3 do not show any significant difference in the charge carrier transport before and after thermal annealing at 200 $^{\circ}$C. The charge carrier mobility in both cases is at the same, relatively low level $\mu= 10^{-5}$ cm^2/Vs. We assumed that this moderate charge carrier mobility likely originates from low molecular arrangement of the polymer backbones in the thin-films (amorphous structure). This in turn may result from relatively long alkyl chains (more than C6) which reduce charge transport in regioregular polythiophene derivatives [A. Babel, S.A. Jenekhe / Synthetic Metals 148 (2005) 169–173]. We conclude that thermal reduction of the substituent length in drop cast film does not improve the charge carrier mobility. The most likely reason for such behavior is the thickness of the semiconducting and consequently a less efficient thermo-cleavage process next to dielectric/semiconductor interface.
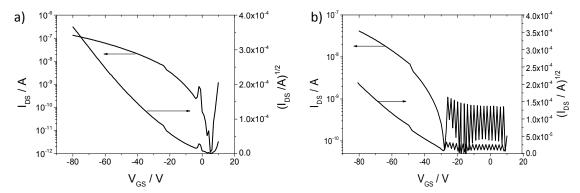

Figure S3. Transfer characteristic at V_{DS} = −80 V for the *poly*-**9a**-based transistors obtained after thermal annealing (a) at 100 °C (12 h) and (b) at 200 °C (1 h).

S4. Organic Solar Cell Fabrication and Characterization

Solar cells were fabricated on indium tin oxide (ITO) coated glass (ShinAn SNP, $R_{sheet} \approx 13$ Ω/sq). The ITO substrates were structured in hydrochloric acid and ultrasonically cleaned in acetone and isopropanol. To polarize the surface and to remove organic residues, the samples were exposed to an oxygen plasma (120 s). After cleaning, the substrates were transferred into a glove box and kept under dry nitrogen atmosphere (<0.1 ppm O$_2$ and H$_2$O) throughout the entire fabrication process. Then, a 20 nm thick layer of low-conductive poly(3,4-ethylenedioxythiophene):polystyrenesulfonate (PEDOT:PSS, Heraeus Clevios VPAI 4083) was spin coated on top. To remove residual water from the PEDOT:PSS layer, the

samples were stored on a hotplate at a temperature of 120°ˆC for 15 min. Subsequently, the active layer comprising a blend of poly-9a and PCBM (Solenne BV, 40 mg/ml, 1:0.5 - 1:1.25) was spin coated from dichlorobenzene. Then the samples were thermally annealed on a hotplate at 150°C and 200°C for 10 minutes, respectively. Finally, the Ca/Al electrodes were evaporated (1 Å s^{-1} and 3Å s^{-1}) through a shadow mask under high vacuum (3x10^{-6} mbar). The current density-voltage (J-V) characteristics were measured with a source measurement unit (Keithley 238) under nitrogen atmosphere. A solar simulator (Oriel 300 W) was used to simulate sunlight according to the ASTM G-173-03 AM1.5 standard. The solar simulator light intensity was monitored with a calibrated spectrometer in order to minimize the spectral mismatch within the relevant wavelength regime.

TOC graphic